N/π AND N/σ INTERACTIONS OF THE AMIDE LINKAGE WITH ITS N-SUBSTITUENTS: A QUANTUM CHEMICAL STUDY

A THESIS
SUBMITTED TO THE DEPARTMENT OF CHEMISTRY
AND THE INSTITUTE OF ENGINEERING AND SCIENCES
OF BILKENT UNIVERSITY
IN PARTIAL FULLFILLMENT OF THE REQUIREMENTS
FOR THE DEGREE OF
MASTER OF SCIENCE

By
ŐZLEM DEMİR

August 2002

I certify that I have read this thesis and in my opinion it is fully adequate, in scope and in quality, as a thesis of the degree of Master of Science.

_____

Assoc. Prof. Andrzej S. Cieplak (Supervisor)

I certify that I have read this thesis and in my opinion it is fully adequate, in scope and in quality, as a thesis of the degree of Master of Science.

_____

Prof. Dr. Şefik Sűzer

I certify that I have read this thesis and in my opinion it is fully adequate, in scope and in quality, as a thesis of the degree of Master of Science.

_____

Assoc. Prof. Ulrike Salzner

I certify that I have read this thesis and in my opinion it is fully adequate, in scope and in quality, as a thesis of the degree of Master of Science.

_____

Prof. Dr. Salim Çıracı

I certify that I have read this thesis and in my opinion it is fully adequate, in scope and in quality, as a thesis of the degree of Master of Science.

_____

Prof. Dr. Engin U. Akkaya

Approved for the Institute of Engineering and Sciences

_____

Prof. Dr. Mehmet Baray

Director of Insitute of Engineering and Sciences

ABSTRACT

N/π AND N/σ INTERACTIONS OF THE AMIDE LINKAGE WITH ITS N-SUBSTITUENTS: A QUANTUM CHEMICAL STUDY

ÖZLEM DEMÍR

M. Sc. in Chemistry

Supervisor: Andrzej S. Cieplak

August 2002

The overall contribution of backbone-backbone H-bonding to the stability of proteins remains an unresolved issue. However, a wealth of spectroscopic, structural, and thermodynamic evidence indicates that the strength of those interactions increases on going from turn or 3_{10}-helix to α-helix to β-sheet. This implies that the electronic properties of the amino acid side chains and their local interactions with the peptide bonds might play a role in secondary structure stability. One such interaction is suggested by the apparent dependence of thermodynamic β-sheet propensities, and of ^{15}N NMR chemical shifts of oligopeptides, on resonance constants of the side chains: electron-density shift from the *i+1* residue into the *i, i+1* peptide bond which would increase basicity of the carbonyl O and thereby strengthen its H-bond. To test this counterintuitive proposition, N/π and N/σ interactions of the amide linkage with its N substituents were investigated. Effects of substitution have been characterized by computational examination of the changes in energy, molecular geometry, electron density distribution, and electronic structure, in three series of compounds: (1) formamides $HC(=X)NY_2$ (X=O, S, Se; Y=H, CH_3, F, Cl, Br); (2) 2,3,-*endo,endo*-disubstituted N-acyl-7-azabicyclo(2.2.1)heptanes and 2,3,-*endo,endo*-disubstituted 7-bicyclo(2.2.1)-heptyl cations; and (3) 3-substituted 5,6-diaza-1-bicyclo(2.1.1)hexyl cations. Both *ab initio* (MP2) and DFT methods were employed using Pople's basis sets (6-31+G(2d), 6-31+G*, and 6-31G*).

N-halo substitution effect on the potential energy surface of simple formamide derivatives is found to be largely related to the electronegativity of the substituents. The exception to this general trend is found in the case of the F effect on the transition structures for inversion, where F lp donation appears to assist π-bonding across the C-N bond, stabilizing the charge polarized resonance form of the amide group. This is supported by the examination of the variation in bond

distances, bond orders, energy and extension of the canonical π-symmetry orbitals, and NBO occupancies of the localized orbitals. On the other hand, the implied π-bonding across the N-F bond is not reflected in the group transfer energies obtained as heats of the isodesmic substitution reaction, the effect being apparently too small in comparison to the total bond energies.

In accord with the experimental data, N-acetyl-7-azabicyclo(2.2.1)heptane is found to be highly pyramidalized on N7. However, due to the very small barrier to inversion, chalcogen substitution, as in N-thioacetyl and N-selenoacetyl- derivatives, results in virtual planarity of the amide N. The planar geometry is readily distorted by remote substitution in 2,3-*endo,endo*-disubstituted N-thioacetyl-7-azabicyclo(2.2.1)-heptanes. The direction of pyramidalization is the same for strongly electron-donating substituents and strongly electron-withdrawing substituents. The dual parameter treatment suggests that in the first case pyramidalization depends largely on the NBO energies of the occupied orbitals of the bicycloheptane C-C bonds, while in the second case both the occupied and vacant orbitals interact with the N center. Examination of the electron density shifts associated with the change in conformation of the π-donor substituents confirms that the thioamide N acts as a resonance acceptor of the σ C-C density.

Finally, 5,6-diaza-1-bicyclo(2.1.1)hexyl cation is found to be an excellent model system to probe π-donor capacity of the range of substituents, including all the coded amni acid side chains, even in their ionized forms. The first scale of substituent constants is obtained to characterize resonance interactions in the σ-bond systems, related to the scale of conventional experimental σ_R constants.

The findings of the present study suggest that the amide linkage can indeed act as a resonance acceptor of π- and σ-density of its N substituents. These results may further our understanding of the local interactions in proteins and the origin of secondary structure propensities of the coded amino acids.

Keywords: Extended hyperconjugation, N-halo substitution, substituent effect, amides, inductive and resonance constants

ŐZET

AMİD BAĞININ
N ATOMUNA BAĞLI GRUPLARLA
N/π VE N/σ ETKİLEŞİMLERİ:
KUANTUM KİMYASAL BİR ÇALIŞMA

ÖZLEM DEMİR

Kimya Bőlűmű Yűksek Lisans

Tez yőneticisi: Andrzej S. Cieplak

Ağustos 2002

Ana zincirler arasındaki hidrojen bağlarının proteinlerin kararlılığına katkısı henüz açıklığa kavuşmamış bir konudur. Ancak, birçok spektroskopik, yapısal ve termodinamik delil bu etkileşimlerin sırasıyla tőrnden sırasıyla 3_{10}-helikse, α-helikse, β-tabakaya giderken daha kuvvetlendiğini gösterir. Bu da aminoasit yan zincirlerinin elekronik özelliklerinin ve bunların peptid bağları ile lokal etkileşimlerinin sekonder yapı kararlılığında rol oynayabileceğine işaret eder. Termodinamik β-tabaka yatkınlıklarının ve oligopeptidlerin ^{15}N NMR kimyasal kaymalarının yan zincirlerin rezonans sabitleri ile değişimi de böylesi bir etkileşimi önerir: *i+1* rezidűsűnden *i, i+1* peptit bağına elektron geçişi, ki bu geçiş karbonil oksijeninin bazlığını artırır ve böylece yaptığı hidrojen bağını kuvvetlendirir. Bu farklı öneriyi test etmek için amid bağının N atomu üzerindeki gruplarla yaptığı N/σ ve N/π etkileşimleri incelendi. N atomu üzerine eklenen grupların etkileri, enerjideki, moleküler geometrideki, elekron dağılımındaki ve elektronik yapıdaki değişimlerin üç seri bileşik için teorik olarak incelenmesiyle karakterize edildi: (1) formamidler HC(=X)NY$_2$ (X=O,S,Se; Y=H, CH$_3$, F, Cl, Br); 2,3-*endo,endo* pozisyonuna ekleme yapılmış N-asil-7-bisiklo(2.2.1)heptil katyonları; ve (3) 3 pozisyonuna ekleme yapılmış 5,6- diaza-1-bisiklo(2.1.1)hekzil katyonları. Hem MP2 hem de YFT (yoğunluk fonksiyonel teori) metotları Pople'nın kullandığı 6-31+G(2d) ,6-31+G* ve 6-31G* ile birlikte kullanıldı.

N atomu üzerine halojen eklemeninbasit formamid türevlerinin potansiyel enerji yüzeyi üzerindeki etkisinin büyük ölçüde eklenen grupların elektronegativitesiyle ilişkili olduğu bulundu.Bu genel durumun istisnası F atomunun çevrilme geçiş yapısı üzerindeki etkisinde görülür, ki F atomu bağ yapmayan elektron çifti amidin yük polarize rezonans formunu

kararlaştırarak C-N bağı üzerindeki π-bağlanmasına yardım ettiği izlenimi doğar. Bu, bağ uzunluklarındaki, bağ sayılarındaki, kanonik π-simetri orbitallerinin enerji ve uzanımlarındaki, lokalize olmuş orbitallerin NBO doluluklarındaki değişimlerle de desteklenir.Ancak, N-F bağı üzerinde öngörülen π- bağlanması, izodesmik yerdeğiştirme tepkimelerinin ısıları olan grup-transfer enerjilerinde yansıtılmaz; etki toplam bağ enerjileriyle karşılaştırılınca çok küçük kalır.

Deneysel datalarla uyumlu olarak, N-asetil-7-azabisiklo(2.2.1)heptan'ın N7 üzerinde oldukça fazla piramidalize olduğu bulundu. Ancak, çok küçük çevrilme enerji bariyeri yüzünden, halojen eklenmesi N-tiyoasetil ve N-selenoasetil türevlerinde olduğu gibi amid N'unun düzlemsel olmasına yol açar. Düzlemsel geometri N-tiyoasetil-7-azabisiklo(2.2.1)heptanlarda 2,3-*endo,endo* pozisyonuna ekleme yapılarak kolayca bozulabilir. Piramidalizasyonun yönü eklenen gruplar kuvvetli elektron verici olsa da, kuvvetli elektron alıcı olsa da aynıdır.

İkili parametre muamelesi, eklenen grupların kuvvetli elektron alıcısı olması durumunda piramidilizasyonun genel olarak bisikloheptan'ın C-C bağlarının dolu orbitallerinin NBO enerjilerine bağlı olduğunu; kuvvetli elektron verici olması durumunda ise hem dolu hem de boş orbitallerin N ile etkileştiğine işaret eder. π-vericisi grupların konformasyonlarının değişimiyle meydana gelen elektron yoğunluğu değişimlerinin incelenmesi, tiyoamiddeki N atomunun σ-C-C elektronlerına karşı elektron alıcısı gibi davrandığını tasdik eder.

Son olarak, 5,6-diaza-1-bisiklo(2.1.1.)hekzil katyonunun kodları bilinen aminoasit yan zincirlerini (hatta onların iyonize formlarını) da kapsayacak şekilde birçok grubun π-vericilik kapasitesini ölçmek için mükemmel bir model sistem bulundu. Konvensiyonel deneysel σ_R sabitlerinin skalasıyla ilgili olarak, σ bağlı sistemlerin rezonans etkileşimlerini karakterize etmek için grup sabitlerinin ilk skalası elde edildi.

Bu çalışmanın sonuçları, amidlerin aslında N atomuna bağlı olan grupların π- ve σ-elektronlarına karşı bir rezonans alıcısı gibi davrandığını gösteriyor. Bu sonuçlar, proteinlerdeki lokal etkileşimlerin ve kodlu aminoasitlerin ikincil yapı yatkınlıklarının sebebinin daha iyi anlaşılmasına katkıda bulunabilir.

Anahtar kelimeler: genişletilmiş hiperconjugasyon, N-halo eklemesi, grup ekleme etkisi, amidler, indűktiv and rezonans sabitleri

To my parents, Asiye and Mehmet
and my sister Gülçin

ACKNOWLEDGEMENT

It is a plesure for me to express my deepest gratitude to Andrzej S. Cieplak for his great help, kindness, support and optimistic approach throughout my studies.

I appreciate kind and valuable help of Dr. Salzner.

I would like to thank dear friends Olga Samarskaya, Ahmet Selim Vakkasoğlu, N. Tuba Gülbağcı, Őzgür Çelik, Onur Atasoylu, Banu Altıntaş, Banu Sűrűcű, Ebru Demir, Erkan Ziya Çiftlikli, Çağrı Ateşin, Hüseyin Karakuş for their help and continuous support.

I am also thankful to the Head of the Deapartment, Şefik Sűzer, and all past and present members of the Chemistry Department.

TABLE OF CONTENTS

LIST OF TABLES

LIST OF FIGURES

1. Introduction

As pointed out by Bent,[1] gas-phase geometries of simple amides and esters do not support Pauling's resonance model which implies large contributions of the polar canonical forms N^{+}=C-O^{-} and O^{+}=C-O^{-} in their structures.[2]

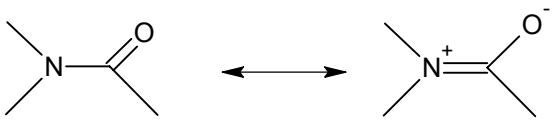

I **II**

Scheme 1

Contrary to expectations, the C=O bond distances in such molecules are similar to the ones found in simple aldehydes and ketones. An explanation of this fact has been proposed by Wiberg and Laidig, who carried out an extensive computational study of the internal rotation in amides.[3] These authors suggested that the C=O bond length of formamide is relatively unaffected by rotation for two reasons. Firstly, this bond is highly polarized even in the rotated saddle-point structures, and the carbonyl O appears very nearly saturated with electron density, so increasing its electronic population does not give it extra stability. In Wiberg's view, the formamide structure is adequately represented by the polar Lewis structure that does not involve π-bonding on the C-N bond.[3a]

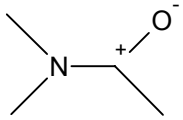

III

Scheme 2

Secondly, while the oxygen does gain some π-electron density on going from the twisted to planar forms, it loses σ-electron density. The loss occurs because of the increase in electronegativity of the formamide nitrogen resulting from a change in hybridization, i.e. due to increased polarization of the C-N and C-O σ-bonds.

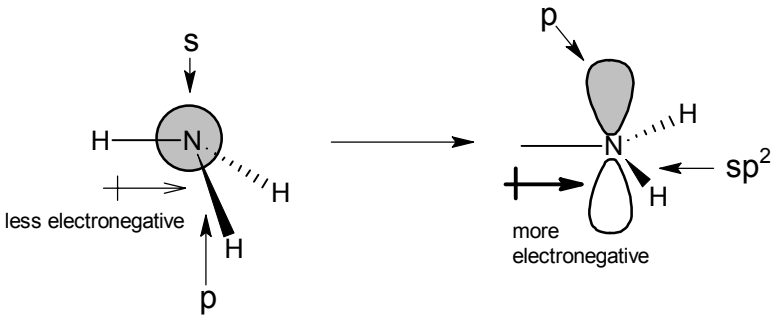

Scheme 3

Somewhat later, Glendening et al have emphasized yet another interaction which would improve upon this rehybridization and lead to a loss of charge density from the carbonyl O: the O $2p_y$ unshared electron pair delocalization into the C-N bond (in the plane of the σ-framework).[4]

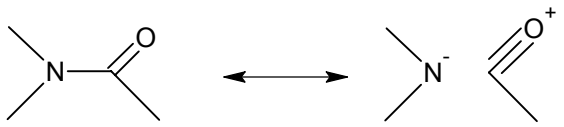

I **IV**

Scheme 4

Thus, in formamide, the effect of resonance is weak and offset by consequences of rehybridization. While the magnitude of the concomitant σ-density shift is debatable,[5] the effect seems considerable and usually rather underestimated in the theory of organic structure and reactivity. Is it, however, also true in the case of the more substituted amides, lactams, peptides? The question as to whether and how the relative importance of resonance and rehybridization in amides varies upon substitution has been subsequently addressed by regression and principal component analyses of internal coordinates for the carboxamide groups in the crystal structures.[6] The study found three patterns of coupling of the *r*(C=O), *r*(C-N), $|\theta_N|$ coordinates, which indeed appear to be related to the major types of the amide substitution. A hypothesis explaining this diversity was based on the assumption that the observed structural variation maps out initial stages of rehybridization accompanying internal rotation; that is, the amide bonds in the crystal structures deform along the rehybridization/rotation path.

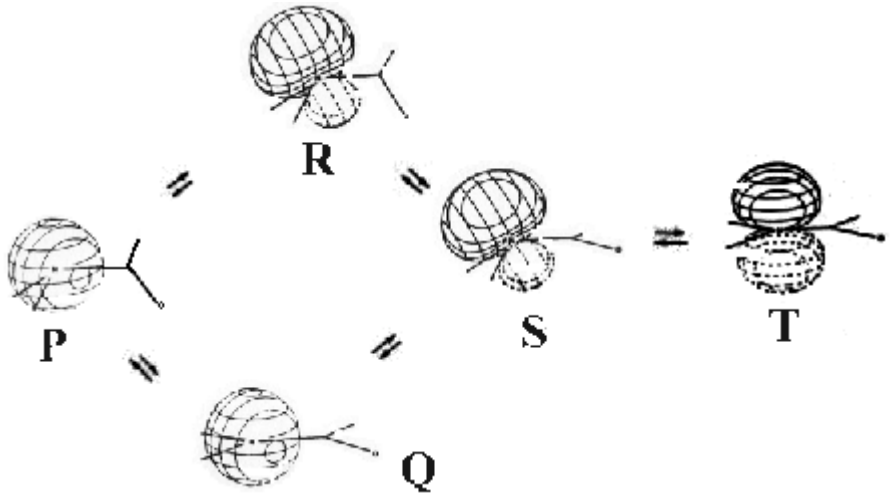

Figure 1: Proposed path for the internal rotation and rehybridization of the amide bonds

The position of the minimum and the saddle point along this path (the actual electronic configurations of the amide linkage) would depend on molecular embedding (e.g. alkyl substitution, lactam-ring size) and lattice interactions (e.g. H-bonding). In other words, the amide linkage should not be thought of in terms of a single standard resonance hybrid, but rather in terms of a spectrum of structures along the rehybridization/polarization path. A change in substitution or intermolecular interactions might shift the electronic configuration of a given amide bond from one region of this path to another, and Wiberg's and Pauling's

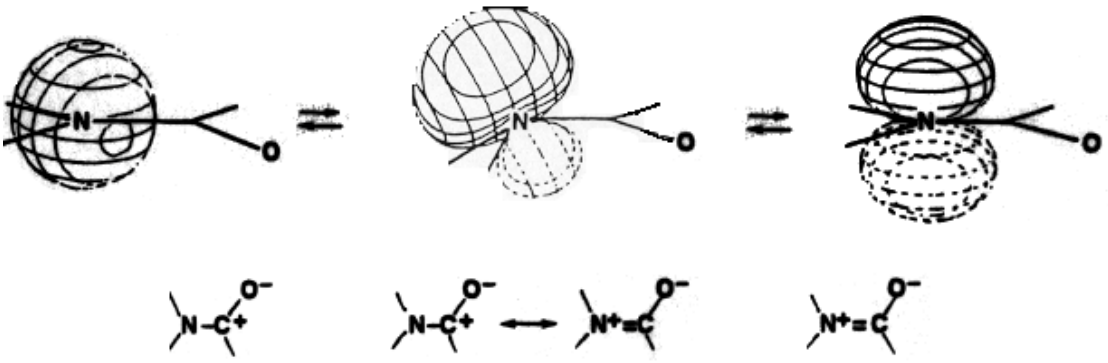

Wiberg configuration **Pauling configuration**

Figure 2: Rehybridization/ polarization path

models would represent the limiting structures of the entire path.

The above model of electronic structure of the carboxamide linkage provides a useful framework to discuss the role of backbone-backbone H-bonding in stabilization of the secondary structure of proteins, and in folding in general. The overall contribution of hydrogen bonds to the stability of proteins remains an unresolved issue, with backbone H-bonding described as being both stabilizing, and net destabilizing:[7] the exact nature and magnitude of the contributions of these interactions to protein folding reactions have been difficult to determine experimentally. However, the structural, spectroscopic, and thermodynamic evidences suggest that the strength of backbone H-bonds increases on going from turn or 3_{10}-helix to α-helix to β-sheet. Thus, $^{3h}J_{NiC'j}$ interactions across those bonds,[8, 9] recently reported to correlate with hydrogen bond distances,[10] with isotropic N_i-H chemical shifts,[8] and with $^{1}J_{NiC'i}$ couplings,[11] tend to be greater for β-sheet H-bonds than for α-helix H-bonds, and have not been observed in 3_{10}-helices.[9] This is consistent with early conclusions of the surveys of H-bonding geometry in ultrahigh resolution crystal structures of proteins,[12, 13] with trends in amide I and amide III band shifts in IR,[14] and with the results of thermochemical analyses of proteins.[15] The issue of the role of backbone interactions was also addressed using unnatural amino acid mutagenesis.[16-20] In such studies α-hydroxy acids have been incoporated into the polypeptide chain via specialized in vitro translation technique, by solid-phase peptide synthesis, or by an enzymatic-chemical semisynthesis.[21] The resulting replacement of the peptide linkage NH group with the ester linkage O potentially removes one H-bond and weakens the other due to lower basicity of the ester carbonyl group compared to the amide carbonyl group. The substitutions in the peptide bonds which are H-bond acceptors in α-helix 39-50 in T4 lysozyme and an antiparallel β-sheet (two edge-strand positions) in the five-stranded β-barrel of staphylococcal nuclease were found to be destabilizing by 0.9 and 1.5-2.5 kcal mol^{-1} with respect to wild type enzymes. This appears consistent with the other observations, but of course the experimental ΔΔG° measured upon deleting or perturbing one member of a hydrogen bond pair does not provide a measure of the strength of a hydrogen bond. Rather, the ΔΔG° reflects in this case the difference between the amide interactions in the folded and unfolded states and the ester interactions in the folded and unfolded states, all in water. A number of assumptions concerning solvation energies, the degree of solvent accessibility at the site of mutation, as well as other dipole-dipole interactions in the local protein environment, are necessary to interpret the magnitude of the destabilization effect.

Recently, however, the approach of single-site mutation: peptide → depsipeptide has been applied in a computational gas-phase study.[22] Full optimizations of a series of N-acetyl polyalanyl amides (AcNH-Ala$_n$-NH$_2$, n=6-14) in helical (2_7-, 3_{10}-, 4_{13}- and a 'hybrid' κ-helix) and hairpin (two- and three-stranded antiparallel β-sheets) conformations were carried out at the HF/3-21G level of theory to probe capacity of the simple *ab initio* method to reproduce local minima geometries and general shape of the potential energy surface. Subsequently, in eight representative conformers, each residue was substituted, one at a time, with L-lactic acid (single-site mutations of AcNH-A$_n$-NH$_2$, mA → Lac, m = 1, … n; replacing peptide NH with O). The resulting mutant structures were fully optimized, and group transfer energies ΔE_{GT} were obtained as heats of the isodesmic reactions AcNH-A$_n$-NH$_2$ + AcOMe → AcNH-A$_x$(Lac)A$_y$-NH$_2$ + AcNHMe (x, y = 0, … n−1) which are nearly thermoneutral for Ala-Ala peptide linkages not involved in H-bonds. Examination of the integrity of H-bonding pattern and ψ_i, ϕ_i distribution identified several mutants with significant distortions of the 'wild-type' structure (e.g. a transition from i, i+3 to i, i+4 H-bonding). For all the other mutants, the group transfer energies were found to correlate with the degree of charge polarization of the parent peptide linkages as measured by the difference in Mulliken populations at H and O in H-N-C=O. Thus, the described approach provides the first quantitative appraisal of how the conformation of polypeptide chains and extension of the H-bonding network affect the strength of backbone-backbone C=O···H-N bonds. In accordance with all the previously quoted data, the results support the notion that the strength of those bonds tends to increase on going from 3_{10}-helix to α-helix to β-sheet.

Since amide groups involved in stronger H-bonds are more charge polarized, i.e. the resonance contribution in their structure increases, the change in electronic configuration of peptide bonds in 3_{10}-helix, α-helix, and β-sheet corresponds to the shift from Wiberg to Pauling configuration along the rehybridization/polarization path.

The above hypothesis implies that the electronic properties of the side chains might play a role in secondary structure stability. Certainly, the side-chain inductive effect can make a neighboring C=O a better or poorer Lewis base, and a neighboring N-H a better or poorer Lewis acid. However, the resonance effect of the C_β substituents in the Ala* amino acid side chains might also be important (Ala* = coded amino acids other than Gly and Pro). Recently,

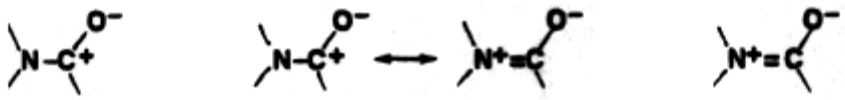

Wiberg configuration **Pauling configuration**

Turn **Helix** **Strand**

Figure 3: The change in electronic configuration of peptide bonds

one-bond C_α-C_β coupling constants in ^{13}C NMR were reported to depend on conformation,[23] and such a dependence is commonly interpreted as a result of hyperconjugative interactions.[24] Furthermore, it has been observed that the thermodynamic secondary structure propensities for α-helix correlate with the average ^{13}C NMR chemical shifts for the carbonyl C' in protein α-helices.[25] Since the chemical shifts of the trigonal C mostly depend on the paramagnetic term, and therefore on the occupancy of the $2p_z$ orbital, it seems likely that this correlation is due to hyperconjugation between the peptide bonds and the side chain C_α-C_β bonds.[26]

In 1994, two independent studies of the effect of single site mutations on free energy of folding of B1 domain of streptococcal protein G have established the first thermodynamic scale of β-sheet propensities for a central strand, and an analogical scale for the edge strand in the same protein was reported shortly thereafter.[27-29] The β-sheet propensities obtained for the B1 domain were shown to correlate with the resonance constants σ_R of the side-chain moieties attached to C_β of Ala* amino acids.[25,30] One possible way to explain this correlation is to assume that the side chain-peptide bond hyperconjugation in the extended strand increases basicity of the peptide bonds and thereby the stability of hydrogen bonding in the β-sheet. Such explanation is consistent with the fact that the ^{15}N NMR chemical shifts of simple N-acetylated amino acids in DMSO[31] also correlate with the side-chain inductive and resonance constants (σ_I and σ_R) and the dependence is quite similar to that found for the for the edge-strand β-sheet propensities.[25, 30]

In terms of the rehybridization/polarization-path model, this explanation assumes that even σ-bonds attached to C_α at the N terminus of the peptide linkage can interact with the nitrogen center as resonance donors (π-donors), and thereby stabilize that peptide linkage in

its polar form, shifting its electronic configuration towards the strand configuration. For most chemists, this must be a somewhat counterintuitive proposition, given the presence of an unshared electron pair on the nitrogen in the main canonical Lewis structure of the carboxamide group, and presumably weak π-donor capacity of the C_α-C_β bonds. Therefore, we decided to examine the N/π and N/σ interactions of the amide linkage with its N-substituents, as well as the resonance donor capacity of the amino acid side chains. The results of such a study should contribute to our understanding of the origin of secondary structure propensities of the coded amino acids.

2. Specific Aims

To gauge the electron density shift from the N-substituents of the amide linkage into its π-orbital system, one can examine how a given N-substitution fragment responds to a shift of the amide configuration along the rehybridization/polarization path, i.e. to the increasing charge depletion at the amide N. As was mentioned, such a shift would occur for instance when the amide becomes an acceptor of a hydrogen bond. A simpler way to achieve the same effect, however, both from the experimental and computational point of view, is to substitute the amide O with S and Se.

To create a fragment with the potential N/π-donor interactions, the carboxamide N-H can be substituted with halogen atoms. Fluorine has been found to be a weak π-donor towards rather electron-deficient centers,[32] but any other substitution would introduce additional degrees of freedom (rotation for OR, rotation and inversion for NR_2). π–Donor capacity is expected to further decrease on going down the group, for chlorine and bromine, due to the mismatch of orbital symmetry.

Examination of the N/σ-interactions requires the use of a conformationally fixed fragment whose σ-bonds would respond to both inductive and resonance effects of the remote substituents. The fragment of 7-azabicyclo(2.2.1)heptane offers those advantages; in addition, the amide nitrogen can be expected to have an increased tendency towards nonplanar equilibrium geometry, and its pyramidalization would provide a valuable probe of the N/σ-interactions.

Thus, this investigation of the N/π and N/σ interactions of the amide linkage with its N-substituents will focus on the computational analysis of variation in geometry, energy, electron density distribution, and electronic structure, in two series of oxo-, thio-, and seleno- amides: N,N-dihaloformamides, and 2,3-*endo,endo*-disubstituted N-acyl-7-azabicyclo(2.2.1)-heptanes.

To assess π-donor capacity of the C_α-C_β bonds of the amino acid side chains, a series of 3-substituted 5,6-diaza-1-bicyclo(2.1.1)hexyl cations will be examined in the same way. In the preliminary investigations, this bridgehead cation structure was found to have both high sensitivity to the extended hyperconjugation effects, and the required stability in the presence of a wide range of donor and acceptor substituents.

3. Literature Background

3.1. Electronic Structure of Amides

The amide group, being a major functional group in organic chemistry, forms the linkage in polypeptides, proteins and various synthetic polymers and has a significant role in determining their special properties. Its planarity and hydrogen bonding propensity are responsible for the formation of secondary and tertiary structures of proteins which lie at the heart of the biological processes. With the increasing interest in biomacromolecules, it became crucial to understand the structure, bonding and electronic properties of the amide group. A detailed knowledge about the amide group will be a guide in making required subtle changes in natural proteins (e.g. by just making point mutations) and to design new materials mimicking biomolecules.

The conventional amide resonance model suggests contribution of two canonical forms: the Lewis structure (I) and the dipolar form (II) as shown earlier in Scheme 1. The dipolar form represents the delocalization of the N lone pair (*lp*) to the C=O $\pi*$ orbital. Therefore, the model implies a charge transfer from N to O, reduction of the C=O bond order, increase in the C-N bond order and the presence of a rotational barrier around the C-N bond.

Most experimental data corroborate the conventional amide resonance model. X- ray crystallography and electron diffraction data[33-41] show that many amides are exactly or approximately planar at the amide nitrogen despite the fact that nitrogen generally prefers a pyramidal geometry as in ammonia. This shows that nitrogen adopts to sp^2-hybridization placing its unshared electron pair in a pure p-orbital, which has the appropriate symmetry for interaction, with the electron-deficient carbon atom at the expense of losing the local stabilization of the lone pair electrons in the pyramidal geometry. The interaction is reflected by the considerable C-N rotational barrier of amides (ΔG=15-21 kcal/mol).[42-48] The rotational barriers of amides are found to increase with increasing dielectric constant of the solvent[47-49], which proves that the ground state structure is more polar and thus, more favored by polar solvents compared to the transition state structure. The effect of rotation about the C-N bond has been studied by using IR[50], UV[51], ^{1}H NMR[52], ^{13}C NMR[53], and ^{15}N NMR[43] spectroscopies and ESCA.[54] The results correlate well with the reduction of amide resonance during C-N bond rotation.

Despite being able to rationalize a lot of experimental results, simple amide resonance

model is just a qualitative model, and as such, has some failures including the unexpectedly small C=O bond length change mentioned. In particular, the fact that thioamides have larger rotational barriers than the analogous oxoamides[47] is anomalous from the point of view of the simple amide resonance model. The model would predict larger rotational barriers for oxoamides than thioamides, since one would anticipate O, being more electronegative than S, to facilitate more delocalization of N unshared electron pair to the carbonyl group.

Searching for an explanation for larger rotational barriers of thioamides, Wiberg, Laidig and coworkers[3,48,55-59] have challenged the conventional amide resonance model. Their computational studies based on the investigation of planar (**1**) and twisted (**2**) geometries of formamide with Bader's Atoms In Molecules (AIM) method[60] revealed that charge transfer

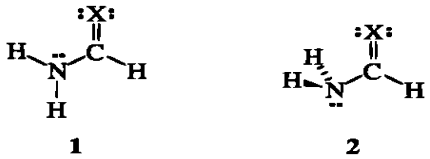

1 **2**

Scheme 5

occurs only between C and N upon rotation, with O being a mere "spectator". Consequently, Laidig and Cameron[59] developed an alternative model based on stabilization/destabilization of the amide nitrogen to replace the resonance view. On the other hand, Wiberg and Rablen[58] reported a significant transfer of π electron density from N to S in thioformamide and claimed that the amide resonance view is more appropriate to describe thioamides than oxoamides.

Recently, Glendening et al[4] came out with an elegant explanation for the controversy about thioamides. This systematic study based on Weinhold's Natural Bond Orbital (NBO) methods[61] and Natural Resonance Theory (NRT)[62] included formamide and its chalcogen (S, Se, Te) analogues. The energetic profile of the rotational path from **1** to **2** reveals an increase in the rotational barrier on going from oxo- to telluro- amides (Figure 4), in accordance with the experimental results.

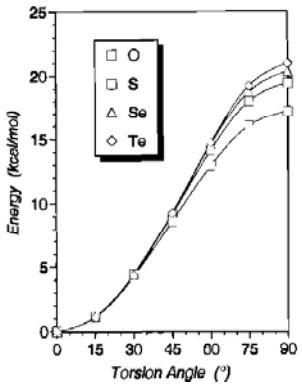

Figure 4: MP2 torsional profiles of formamide and its chalcogen analogues. The 0°and 90° rotamers corespond to **1** and **2**, respectively.

The C-N bond length, which is strongly influenced by rotation, is not only affected by the loss of conjugative interactions but also by concomitant rehybridization of N. A

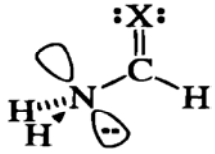

3

Scheme 6

constrained optimization of **3** separates the contributions of the two effects. The difference between **2** and **3** reveals the sole effect of rehybridization as both are devoid of the N $lp \rightarrow \pi^*_{C=X}$ interaction. Table 1 points out that contribution of rehybridization to the CN bond contraction is about one third.

	1	**3**	**2**	Δ(**2**-**1**)	Δ(**2**-**3**)
O	1.362	1.416	1.441	0.079	0.025
S	1.352	1.41	1.438	0.086	0.028
Se	1.347	1.406	1.435	0.088	0.029
Te	1.344	1.406	1.435	0.091	0.029

Table 1: C-N bond lengths of amide conformers in Å

The profile of natural atomic charges during rotation indicates that rotating the twisted (**3**) to the planar (**1**) amide induces a charge transfer from N to the chalcogen. The amides with heavier chalcogens are found to transfer more charge, which implies a larger contribution of

the dipolar form (**II**). This may be thought to be counterintuitive but is corroborated by the higher rotational barriers and shorter C-N bonds of heavier chalcogen analogues. This property is attributed to larger polarizabilities of heavier chalcogens.

Additionally, NRT, which describes a molecule as a weighted sum of all possible resonance structures, is used to elucidate the trend of contribution of **II** upon changing the chalcogen. Table 2 shows how the percentage weight of **II** increases as one goes towards the heavier chalcogens. To elucidate the origin of this trend, the polar covalent character of C=X

structure		X=O	X=S	X=Se	X=Te
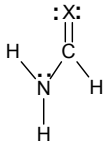	**I**	58,63	58,61	57,13	56,09
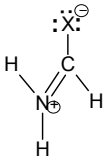	**II**	28,61	29,23	31,01	32,66
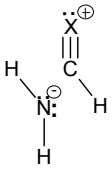	**IV**	3,1	2,8	2,52	2,23
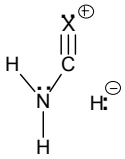	**V**	2,05	1,49	1,23	0,8
others		7,61	7,87	8,11	8,22
bond orders		**X=O**	**X=S**	**X=Se**	**X=Te**
b_{CN}		1,34	1,355	1,381	1,405
b_{CX}		1,717	1,694	1,664	1,636

Table 2: MP2 natural resonance weights and bond orders for formamide and its chalcogen analogues

NBOs of planar(**1**) and twisted(**2**) amides is examined in comparison to the formaldehyde analogues **4** (Figure 5). Unlike $\sigma_{C=X}$ bond, the polarization of $\pi_{C=X}$ bond is strongly influenced

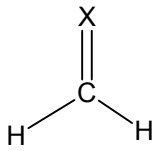

4

Scheme7

by the orientation of the N lone pair. Figure 5 also reveals a significant polarization difference between amides including π-conjugation of N lone pair (**1**) and amides deprived of it (**2**). In fact, the polarization of **2** follows a very similar trend to that of **4**, which does not have N. It is also worth to note that the difference between $\pi_{C=X}$ polarizations of **1** and **2** is apparently larger for heavier chalcogens (Figure 5). Polarization of $\pi_{C=X}$ orbital of **1** towards the chalcogen polarizes the $\pi^*_{C=X}$ orbital in the reverse direction, namely towards the C atom. This makes the $\pi^*_{C=X}$ orbital a better acceptor for resonance interaction N *lp* $\rightarrow \pi^*_{C=X}$. Therefore, the better polarizability of heavier chalcogens facilitates repolarization and leads to enhanced resonance stabilization.

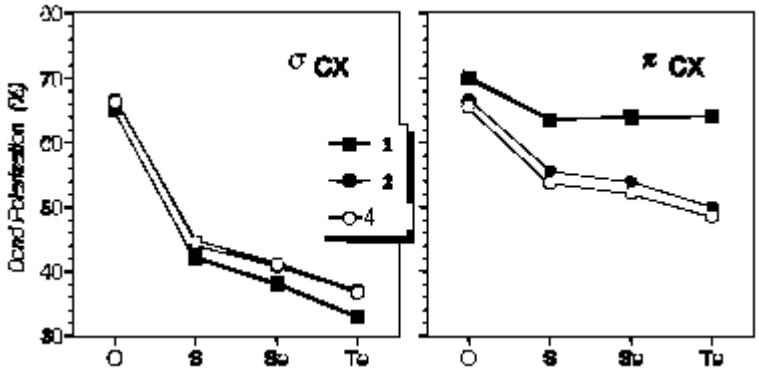

Figure 5: Polarizations of the σ_{CX} and π_{CX} NBOs for planar (**1**) and twisted (**2**) amides and aldehyde analogues (**4**) where X= O, S, Se, Te

Based on all these, one can say that the replacement of a chalcogen with a heavier one in an amide will mimic the polarization effect of involvement of that amide in a stronger H-bond. Thus, substitution of amide O with heavier chalcogens can be used in both experimental and computational studies to probe the effect of increasing the strength of H-bonding.

3.2. Hyperconjugative Interactions in Bicyclo(2.2.1) heptanes and 7-Azabicyclo-(2.2.1)heptanes

A number of experimental observations suggest that the Y center in the 7-Y-bicyclo(2.2.1)heptyl derivatives ($Y=C^{+}R$, NR, $C=CR_2$, C=O etc):

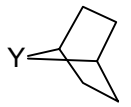

5

Scheme 7

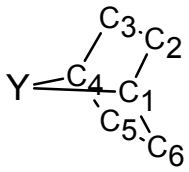

can interact hyperconjugatively with the σ C-C bonds. In the case of the trigonal centers Y, the interactions with the top and bottom C-C bond pairs (C1-C2 & C4-C3 bonds and C1-C6 & C4-C5 bonds, respectively) are equivalent, but this symmetry can easily be perturbed by the remote substitution at one of the bridges (2,3-*endo, endo).* Due to the rigidity of the bicyclo(2.2.1)heptyl skeleton, such substitution does not alter the geometry and steric interactions around Y. The major effect will be the change in capacity of the C-C bonds to act as donors and/or acceptors in hyperconjugative interactions with the Y center. There is some evidence to expect that the C-C bond properties in this skeleton are sensitive to both inductive and resonance effects (extended hyperconjugation, *vide infra*) of the substituents. Furthermore, the angle strain at the one-atom bridge is increased when Y is trigonal planar. The increased strain can be attenuated by pyramidalization, so the planar Y group can be easily distorted out of planarity. If such distortion would be stabilized by hyperconjugation, it may serve as a probe of the interactions with the C-C bonds. The following two sections will review some of the evidence to support these expectations.

3.2.1. Molecular Geometry of 7-Azabicyclo(2.2.1)heptyl derivatives

Crystal structures of some 7-azabicyclo(2.2.1)heptanes have been examined by Ohwada et al.[63] Structures of **8a, 8b** and **9** have been determined by crystallography and compared with their monocyclic analogues **6** and **7.** Table 3 presents the data about pyramidalization of the amide nitrogen: the sum of the three valence angles around the nitrogen (θ) and the out-of-plane

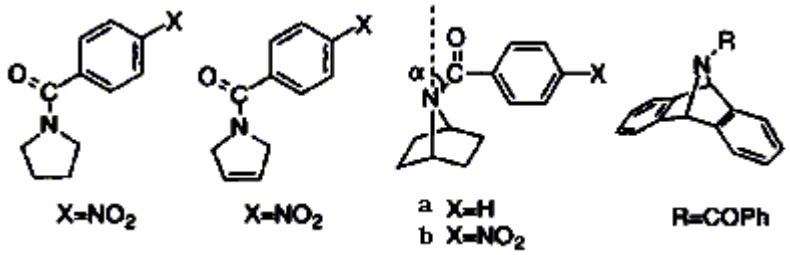

6 **7** **8** **9**

Scheme 8

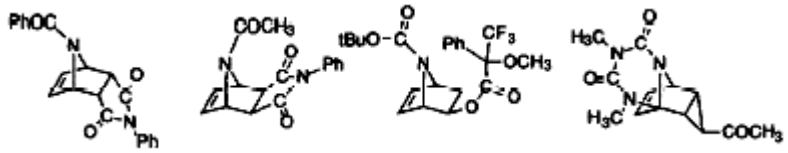

10 **11** **12** **13**

Scheme 9

	angles around N θ (deg.)	out-of-plane angle α (deg.)	N-C bond length (Å)
6	359.3 (0.2)	7.5	1.337 (0.002)
7	357.4 (0.3)	14.8	1.345 (0.003)
8a	349.5 (0.2)	26.8	1.356 (0.003)
8b [a]	347.1 (0.3)	29.8	1.354 (0.004)
	350.1 (0.3)	26.2	1.350 (0.004)
9	347.5 (0.3)	29.4	1.343 (0.004)
10	343.7 (0.5)	33.4	1.353 (0.008)
11	351.2 (0.4)	24.3	1.374 (0.007)
12	339.1	39.1	1.357
13	328.7	47.9	1.382

Table 3: Nitrogen pyramidalization of amides (in degrees) a: Two independent molecules are present in a unit cell.

angle of the substituent on N with respect to the plane formed by N and its two neighbouring C atoms (α). The table indicates nearly planar geometries for monocyclic amides **1** and **2** but highly pyramidalized N atoms for bicyclic **8a, 8b** and **9**. The fact that there is no steric reasons for these three molecules to tilt raises the question of intrinsic pyramidalization for N-acyl-7-azabicyclo(2.2.1)heptanes. To compare recent data with previous ones, the Cambridge Structural Database has been searched for similar structures. The amide derivatives of 7-azabicyclo(2.2.1)heptane, **10-13**, found there had also pyramidal N atoms (Table 3). As these structures have either a bulky appendant or an additional ring, it is easy for one to relate the pyramidalization with steric effects. However, the pyramidalization observed for structures **8a, 8b** and **9,** which are free from steric bias, call for intrinsic pyramidalization of the 7-azabicyclo(2.2.1)heptane motif. Additionally, the carbonyl carbons of the amides **8a, 8b** and **9** as well as those of the monocyclic amides **6** and **7** are found to be perfectly trigonal planar. This proves that the main reason of the non-planarity of 7-azabicyclo(2.2.1)heptane motif is the pyramidalization of the amide nitrogen.

In a subsequent study, Ohwada et al.[64] have investigated the structures of similar molecules: sulfonamides of 7-azabicyclo(2.2.1)heptanes. Similar parameters to those in ref. [63] are used to measure the pyramidalization and the sulfonamides found in the Cambridge Structural Database have been investigated. The obtained 349 examples had an average θ value of 352.4° (with a range of 332.2°-360°), suggesting a general tendency of sulfonamides to pyramidalize. The crystal structures of **14-21** have been determined and their pyramidalization

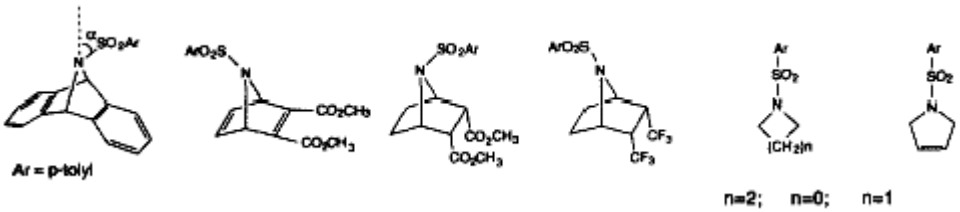

14 **15** **16** **17** **18** **20** **21** **19**

Scheme 10

	angles around N θ (deg.)	out-of-plane angle α (deg.)	N-S bond length (Å)
14	341.4 (2)	36.0	1.628 (3)
15	341.3 (2)	35.9	1.633 (3)
16[a]	336.4 (6)	41.1	1.635 (7)
	336.7 (6)	40.6	1.636 (7)
17	347.8 (2)	29.1	1.627 (3)
18	349.2 (3)	30.4	1.613 (3)
19	353.4 (3)	23.7	1.597 (4)
20[a]	291.2 (2)	59.5	1.649 (3)
	291.3 (3)	59.1	1.647 (3)
21	338.8 (1)	37.3	1.620 (2)

Table 4: Nitrogen pyramidalization of sulfonamides. a : Two independent molecules are present in a unit cell.

data are presented in Table 4.[64] Simple monocyclic sulfonamides **13** and **14** are found to be highly pyramidalized (**18**: θ =349.2°, α =30.4°; **19**: θ =353.4°, α =23.7° shown in Table 2), much more than the corresponding amides **6** and **7** (**6**: θ =359.3°, α =7.5°; **7**: θ =357.4°, α =14.8°). As the planarity of N is attributed to the interaction of its unshared electron pair with S in sulfonamides, the π-bonding of N and S in sulfonamides must be weaker than that of N and C in amides.

It is worth to note that the pyramidalization values of bicyclic structures **14-21** are comparable to (some are even larger than) those of monocyclic analogues **18-21**. And these structures **14-21** would lie among the most pyramidalized sulfonamides if placed in the range obtained from Cambridge Structural Database. It should also be noticed that the direction of tilt of sulfonyl group with respect to the nitrogen trigonal plane changes with different substituents on the substrate as in **15, 16** and **17**.

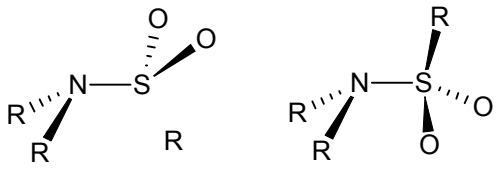

(a) (b)

Scheme 11

Additionally, it is observed that S-C bond places itself either *anti*-periplanar (as in **14, 15, 17, 21**) or *syn*-periplanar (as in **16** and **20**) with respect to the N *lp* (Scheme 11,b and a, respectively). These conformational preferences have been attributed to negative hyperconjugation from N *lp* to the antibonding orbital of C-S bond.[65] Reorientation of the N *lp* increases its electron-donating ability and favors negative hyperconjugation. Parallel with the reorientation, rehybridization of N occurs, and N becomes more like sp^3-hybridized. This increases the p-character of σ bonds of N and thus results in longer bonds (esp. N-S bond). Despite the attenuation of negative hyperconjugation due to elongation of N-S bonds, the reorientation of the N *lp* counterbalances this effect. Thus, the 7-azabicyclo(2.2.1)heptane motif favors nitrogen pyramidalization of N-sulfonamides as well.

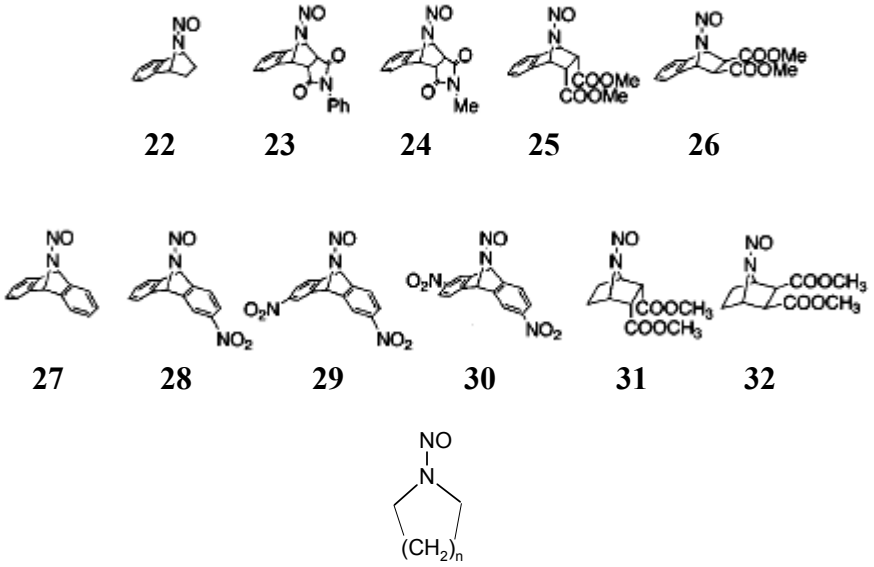

Scheme12

Another example comes from a study of N-NO bond cleavage of N-nitrosamines.[66,67] Having in mind the weakened N-S and N-C bonds in N-sulfonyl and N-acyl 7-azabicyclo(2.2.1) heptanes due to pyramidalization of N, Ohwada and coworkers[66] attempted to use N-nitroso derivatives of 7-azabicyclo(2.2.1)heptanes as potential NO/NO^+ donors. N-nitroso compounds are similar to amides in the presence of resonance interaction and subsequent rotational barriers around N-NO bond which are comparable to those of amides.[68-71] Thus, they are generally found

to be planar like amides. However, the rotational barriers of N-nitoso derivatives of 7-azabicyclo(2.2.1)heptanes are determined to be ~15 kcal/mol which is lower than the ~20 kcal/mol rotational barrier of monocyclic N-nitrosamines.[68,69,72,73] In accordance with the magnitudes of rotational barriers, N-nitroso derivatives of 7-azabicyclo(2.2.1)heptane are found to be very good NO donors (even superior to the widely used NO donors) in solution while the monocyclic N-nitrosamines did not cause any significant NO formation. This is explained with the facile cleavage of N-NO bond due to reduction of resonance in the N-NO group of N-nitroso derivatives of 7-azabicyclo(2.2.1)heptane. The crystal structures of the bicyclic N-nitroso compounds in the solid-state also show that N is pyramidalized.[67] This nitrogen pyramidalization is proposed as the reason of the reduction in N-NO resonance in these structures because it makes the orientation of the orbitals inappropriate for resonance interaction. The results of *ab initio* calculations of a number of monocyclic and bicyclic N-nitrosamines revealed a linear correlation between the rotational barrier around N-NO bond and the C-N-C angle, which proves that N-pyramidalization decreases the rotational barrier.

3.2.2. π-Face Selectivity in Reactions of Bicyclo(2.2.1)heptyl Derivatives

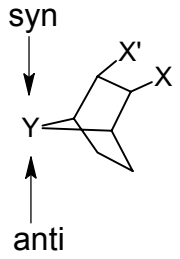

Scheme 13

The π-face selectivity in reactions of bicyclo(2.2.1)heptyl derivatives changes significantly on remote substitution. The syn-preferences in $NaBH_4$ reduction of 2,3-*endo,endo*-disubstituted bicyclo(2.2.1)heptyl derivatives listed in Table 3 form a wide spectrum.[74-80] An attempt to correlate syn-preference with the inductive constants of the remote substituents[30] has proved to be unsuccessfull. However, multiple regression of the same data on both inductive and

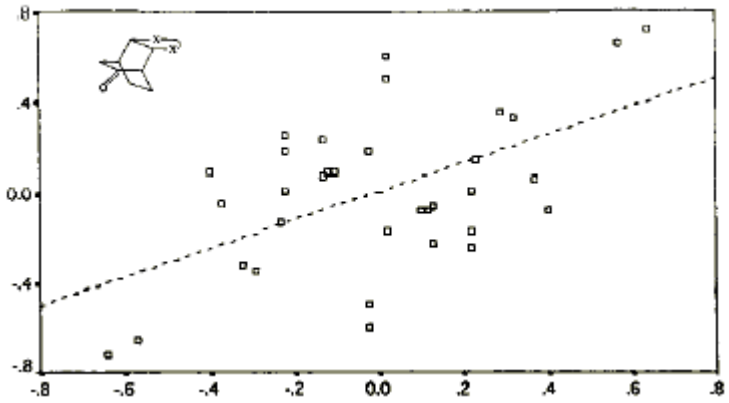

Figure 6: Effect of remote substitution on $NaBH_4$ reductions, log (Z/E) vs. σ_I.

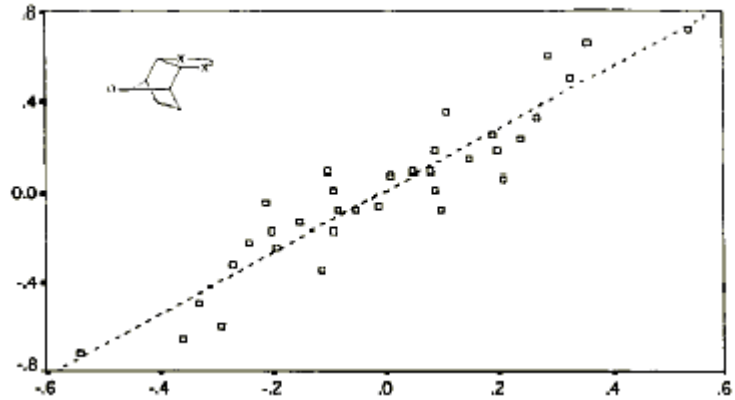

Figure 7: Effect of remote substitution on $NaBH_4$ reductions, log (Z/E) vs.$\lambda\sigma_I+ \sigma_R$

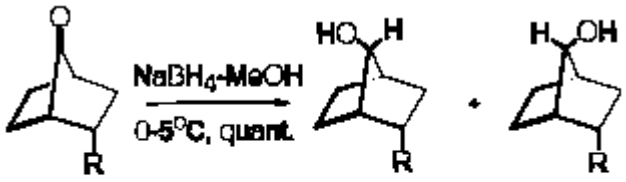

Scheme 14

resonance constants revealed a reasonable correlation, indicating a concomitant contribution of inductive and resonance effects.[30]

Even monosubstitution is found to have strong enough effect to induce diastereoselectivity in $NaBH_4$ reduction of structure **26** (Y=O).[81] Moreover, electrophilic additions to corresponding 2,3-*endo,endo*-disubstituted 7-methylene bicyclo(2.2.1)heptanes exhibits the same selectivity trend.[82]

Some of the experimental studies of diastereoselectivity in reactions of bicyclo(2.2.1)heptane derivatives prompted computational studies to rationalize these results.

Thus, the *anti*-selectivity of 2,3-dimethylbicyclo(2.2.1)heptan-2-one, **33**, is found to be less than that of the 2,3-diethyl analogue **34**,[74-78] e.g. the reaction with $LiAlH_4$ has an *anti/syn* selectivity of 55:45 for the dimethyl derivative and of 79:21 for the diethyl derivative. Yadav et al. investigated the origin of this difference.[79] Optimized geometries show that both **33** and **34**

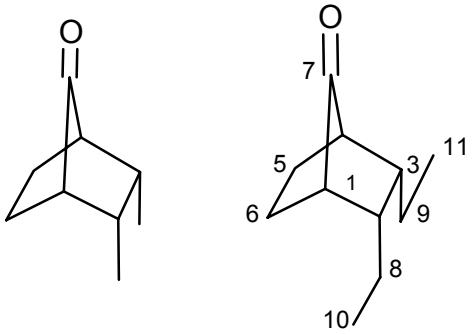

33 **34**

Scheme 15

as well as their cation complexes **33-H$^+$, 33-Li$^+$, 34-H$^+$** and **34-Li$^+$** have O atoms tilted towards the substituted bridge with respect to the plane of C1,C4 and C7, namely *anti*-pyramidalized. Such *anti*-pyramidalization might result in *anti*-selectivity obviously. Thus, calculations predict *anti*-selectivity for reactions of both **33** and **34**. In order to trace the origin of the difference in their *anti*-selectivities, Yadav compared NBO 2nd order perturbation energies of the related interactions. In **33**, one of the three C-H bonds of each methyl group is antiperiplanar to C1-C2/C3-C4 bond and the interaction energy is 3.53 kcal/mol. In **34**, one of the two

methylene hydrogens of each ethyl group is antiperiplanar to the C1-C2/ C3-C4 bond and the interaction energy is 3.93 kcal/mol. These hyperconjugative interactions that increase the electron-donating ability of C1-C2/C3-C4 bonds favor *anti*-pyramidalization. Thus, stronger hyperconjugative interactions in **34** (as well as its cation complexes) might account for the higher *anti*-selectivity of the reaction involving **34**.

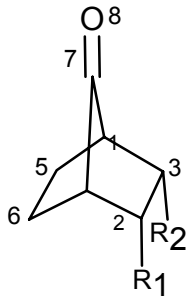

35 : $R_1=R_2= CH_2OMe$

36 : $R_1=R_2= CH=CH_2$

37 : $R_1=R_2= CO_2Me$

Scheme 16

In a similar study,[27] Yadav tried to assess the reason why *anti*-selectivity is observed for **35** and **36** but *syn*-selectivity is observed for **37** although all three are electron-withdrawing substituents.[21, 22] The optimized geometries for **35, 36** and their cation complexes indicate tilt of carbonyl group towards the substituted bridge, predicting their *anti*-preference in reactions. The

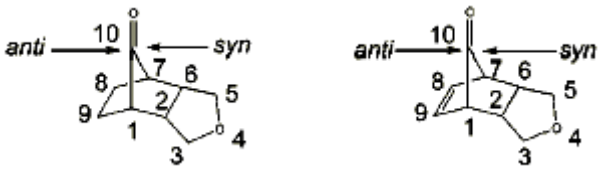

38 **39**

Scheme 17

sum of the NBO 2nd order perturbation energies of σ_{C1-C2}-$\pi^*_{C=O}$ and σ_{C3-C4}- $\pi^*_{C=O}$ interactions is larger than that of σ_{C1-C6}- $\pi^*_{C=O}$ and σ_{C4-C5}- $\pi^*_{C=O}$ interactions, and this is also in favour of *anti*-pyramidalization. The geometry data do not give a clear picture for **37**. However, the analogous interaction energies of **37-2H**$^+$ predict *syn*-selectivity.

A recent study about structures **38** and **39** also suggest operation of extended hyperconjugation.[81] The generally observed anti-selectivity of these structures is related to the interaction of C1-C2 and C6-C7 bonds with C3-H and C5-H bonds which are assisted by the unshared electron pair of the ring oxygen.

3.3 Extended Hyperconjugation

Any type of vicinal secondary bonding interaction (donation from σ, π or n to σ* orbitals; from σ or n to π* orbitals, etc.) is referred to as "hyperconjugation". (Scheme 18) When hyperconjugation is assisted by another donor which has a suitable orientation to interact with the primary donor, the interaction is called "extended hyperconjugation". (Scheme 19)

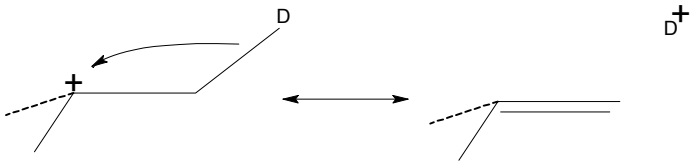

Scheme 18

Scheme 19

Such interactions of orbitals over an intervening σ framework has been known for more than 30 years. The optimal situation for this kind of interactions is a structure having an electron deficient center (e.g. a carbocation) and a highly polarizable and electron-donating substituent. If through-bond inductive effects were the only mechanism for transmission of information, the effects would vanish after 2 intervening bonds. However, substantial effects over three intervening bonds (Si-C-C-X, Sn-C-C-X) have been reported by Lambert et al.[87,]

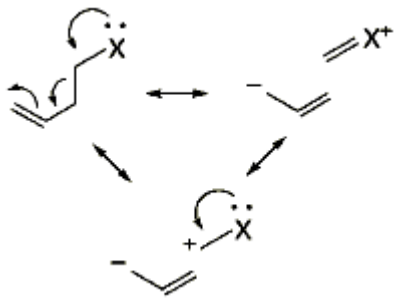

[88] Similar interactions in which

Scheme 20

there exist three or more intervening bonds between the electron deficient center and the substituent (Scheme 20), originally called "double hyperconjugation" by Lambert, [89, 90] are referred to as "extended hyperconjugation" throughout this text. Experimental results which are attributed to extended hyperconjugation will be exemplified in the following section.

3.3.1. Solvolysis Results

Solvolysis of *trans*-4-(trimethylstannyl)cyclohexyl tosylate and *cis*-4-(trimethylstannyl)cyclohexyl tosylate reveal a distinct picture of assistance of extended hyperconjugation.[89] The *trans* stereoisomer has an appropriate arrangement of the Sn-C-C-C-C-X moiety which permits extended hyperconjugation interaction (Scheme 21, a). In order to elucidate relative contributions of carbocation (k_c) and

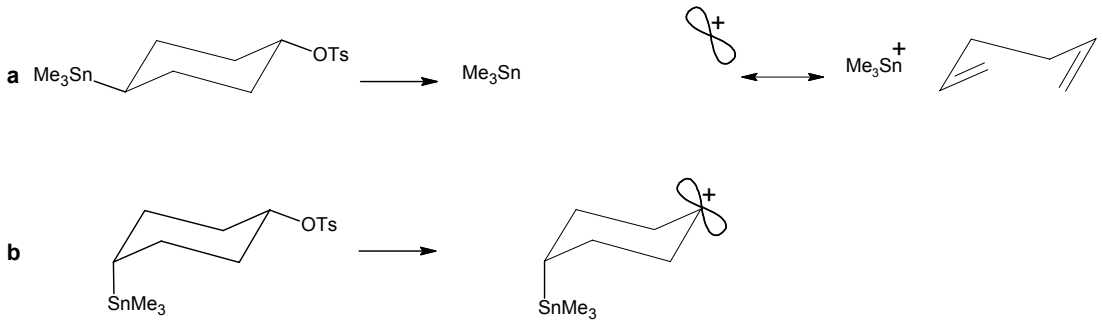

Scheme 21

solvent participation (k_s) mechanisms, solvolysis rates were measured in both ethanol and trifloroethanol at several levels of water content. The values for both *cis* and *trans* isomers were plotted versus the rates of 1-adamantyl bromide according to the procedure of Raber and Harris (Figures 8 and 9). [93]

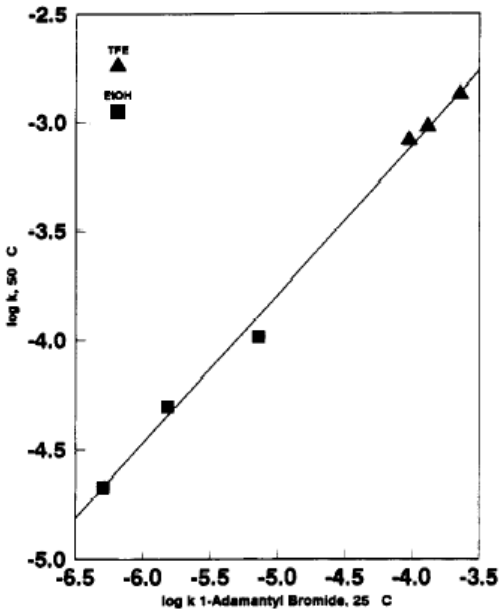

Figure 8:
Raber-Harris plot for *trans* isomer

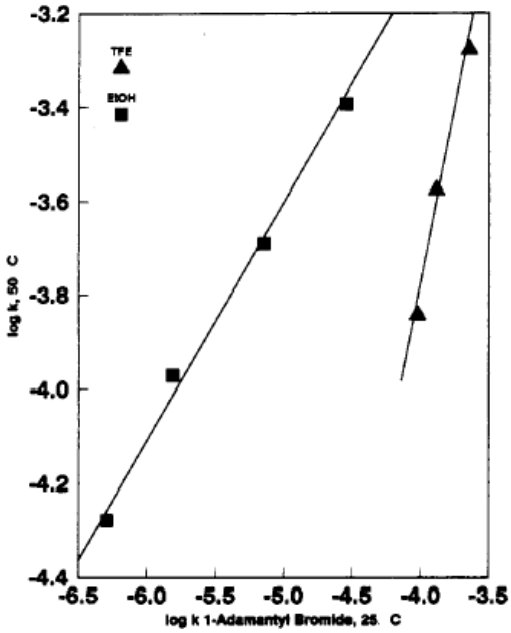

Figure 9:
Raber-Harris plot for *cis* isomer

The Raber-Harris plots (Figures 8 and 9) suggest a solvent assisted (k_s) mechanism for the *cis* isomer (just like cyclohexyl tosylate), but a carbocation (k_c) mechanism for the *trans* isomer. The difference between the two stereoisomers has been attributed to the intramolecular stabilization of carbocation by extended hyperconjugation, decreasing the need for solvent assistance.

3.3.2. Substituent Effects on π-Face Selectivity

Substituent effects on π-face selectivity of numerous reactions (of which 4 examples are explained briefly below) also appear to involve the effect of extended hyperconjugation.

In $LiAlH_4$ reduction of 4-halo-adamantan-2-ones *syn* preference is reported for the 4-iodo compound but *anti* preference for the 4-fluoro compound.[95] The reversal was explained as a result of effective extended hyperconjugation in the case of 4-fluoro compound which makes the substituent a better donor in spite of the high electronegativity of F (Scheme 22).

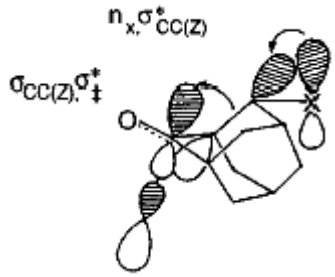

Scheme 22

Syn preference observed with the protic solvent, EtOH changes to *anti* preference with the aprotic solvent, THF in $NaBH_4$ reduction of 5-azaadamantan-2-one (Scheme 23). [91] This reversal in π-face selection was attributed to N *lp* assistance

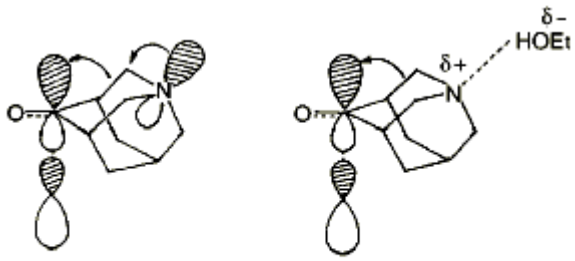

Scheme 23

which is attenuated by H-bonding in the presence of protic solvents like EtOH.[91] Thus, π-face selection dependence on alcohol acidity was proposed to be due to extended hyperconjugation.

Alkylation of β- (2'-tetrahydropyranyl)- and β- (2'-tetrahydrofuranyl)-ester enolates (Scheme 24) which differ only in the ring size has shown significant difference in anti preference (Scheme 24).[92] This difference is proposed to be a result of relatively uneffective O lone pair-$\sigma^*_{C\text{-}C}$ overlap in the five-membered ring compared to that of the six-membered ring, diminishing the O lone pair assistance.

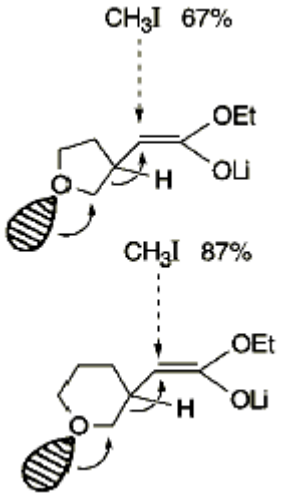

Scheme 24

The π-face selectivity in C-C bond formation in mercaptoisoborneol-based ylide addition to aldehydes is also attributed to the C-S bond hyperconjugation assisted by O lone pair back donation to the $\sigma^*_{C\text{-}S}$ orbital (Scheme 25) .[95] Thus, the *anti* preference decreases when a methylene C replaces O atom in the molecule.

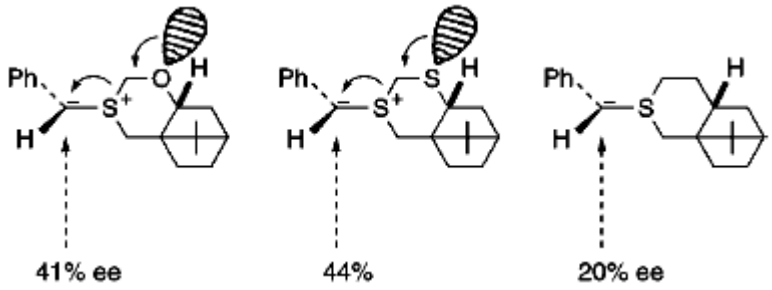

Scheme 25

The importance of conformation of the substituent in hyperconjugative interactions can be seen by comparison of experimental data for structures A and B.[74, 75] (Scheme 26) In structure A, the vinyl group is free to align itself to assist nucleophilic addition hyperconjugatively and thus favors *anti* addition. However, structure B restricts the conformation of the double bond in such a way that it can not participate in hyperconjugative interaction.[94] Therefore, *syn* addition becomes preferred to *anti* addition.

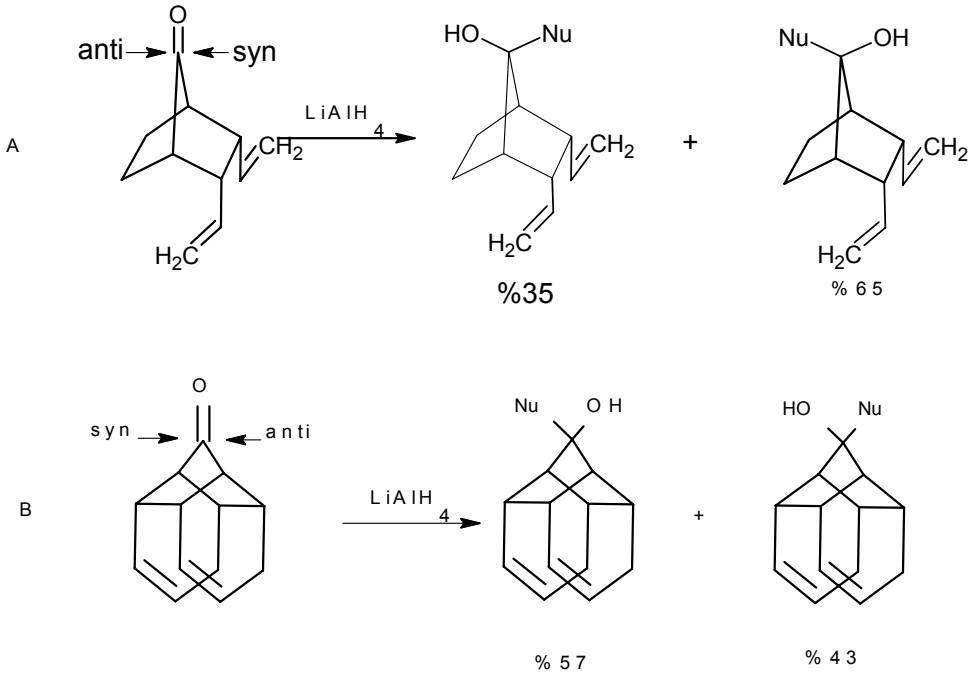
A
O
anti
syn
LiAlH4
CH2
H2C
HO
Nu
%35
Nu
OH
% 65
B
O
syn
anti
LiAlH4
Nu
OH
% 57
HO
Nu
% 43

Scheme 26

3.4. Bridgehead Cations

As mentioned above, carbocations are good probes to examine hyperconjugative interactions since their strong electron demand magnifies the effects. For the bridgehead cations, homohyperconjugative interactions are possible as well as extended hyperconjugation. In extreme cases, those interactions lead to bridging which distorts the geometry significantly. In fact, hyperconjugation and bridging both lie in the spectrum of charge delocalization as different regions and there is no clearcut boundary between them.

The 3,5,7-trimethyl-1-adamantyl cation, **40**, the first alicyclic cation whose structure could be determined,[96,97] adequately exemplifies hyperconjugative interactions in the bridgehead cations. Its crystal structure indicates an apparent contraction of Cα-Cβ bonds (in average) and elongation of Cβ-Cγ bonds (in average) compared to the corresponding reference values.[98] The pyramidalization of C1, i.e. its

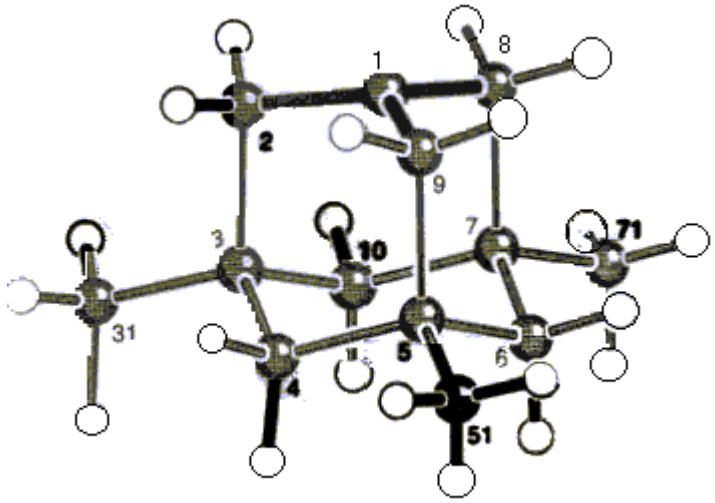

Figure 10 : Crystal structure of **40**

distance from the plane of C2, C8 and C9, is 0.212 Å which is remarkable for an sp^2-like C atom. The average C_β -C_α-$C_{\beta'}$ and C_α-$C_{\beta'}$-Cγ angles also point out the unusual pyramidalization of C1. The quaternary Cγ atoms are slightly flattened except from C_β-Cγ bond: the average C_β-Cγ- $C_{\delta n}$ and C_β-Cγ-$C_{\delta x}$ angles are slightly less and the

$C_\alpha-C_\beta$	1.439(6)	$C_{sp^3}-CH_2-C_{sp^2}$[b]	1.502(1)
$C_\beta-C_\gamma$	1.612(4)	$(C_{sp^3})_3C-CH_2-C_{sp^3}$[b,c]	1.538(1)
$C_\gamma-C_{\delta_n}$	1.527(3)	$(C_{sp^3})_3C-CH_2-C_{sp^3}$[b]	1.538(1)
$C_\gamma-C_{\delta_x}$	1.519(7)	$(C_{sp^3})_3C-CH_3$[b]	1.534(1)
$C_\beta-C_\alpha-C_{\beta'}$	117.9(3)	ideal $C-C_{sp^2}-C$	120
$C_\alpha-C_\beta-C_\gamma$	99.7(2)	ideal $C-C_{sp^3}-C$	109.5[d]
$C_\beta-C_\gamma-C_{\delta_n}$	107.4(2)	ideal $C-C_{sp^3}-C$	109.5[d]
$C_\beta-C_\gamma-C_{\delta_x}$	107.4(2)	ideal $C-C_{sp^3}-C$	109.5[d]
$C_{\delta_n}-C_\gamma-C_{\delta_n'}$	110.9(4)	ideal $C-C_{sp^3}-C$	109.5[d]
$C_{\delta_n}-C_\gamma-C_{\delta_x}$	112.2(2)	ideal $C-C_{sp^3}-C$	109.5[d]
$\lvert C_\gamma-C_{\delta_n}-C_\gamma-C_{\delta_n'}\rvert$	56.2(3)	(e.g., diamond lattice)	60
$\lvert\Delta(C_\gamma)\rvert$[e]	0.454(3)	$^1/_3 \times C_{sp^3}-C_{sp^3}$[b,f]	0.510

[a] Lengths are given in Å, angles in deg. [b] Taken from ref [c] The required reference parameter $(C_{sp^3})_3C-CH_2-C_{sp^2}$ is not available. [d] $\arccos(-^1/_3)$. [e] Bond partners: C_{δ_n}, $C_{\delta_n'}$, C_{δ_x}. [f] Ideal $\Delta(C_{sp^3})$ using three bonds.

Table 5 : Average structural parameters of **40** and corresponding reference parameters

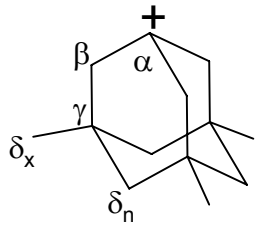

40

Scheme 27

average Cγ- $C_{\delta n}$ -$C_{\delta n'}$ and $C_{\delta n}$- Cγ- $C_{\delta x}$ angles are slightly higher than 109.5°. All these structural features are in accordance with the presence of a C-C hyperconjugative interaction shown in Scheme 28.

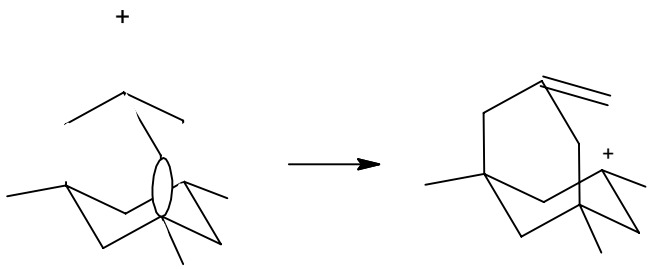

Scheme 28

In a similar fashion, 1,2,4,7-anti-tetramethyl-2-norbornyl cation, **41** is the first bridged cation whose structure could be determined.[99, 100] Due to bridging, its

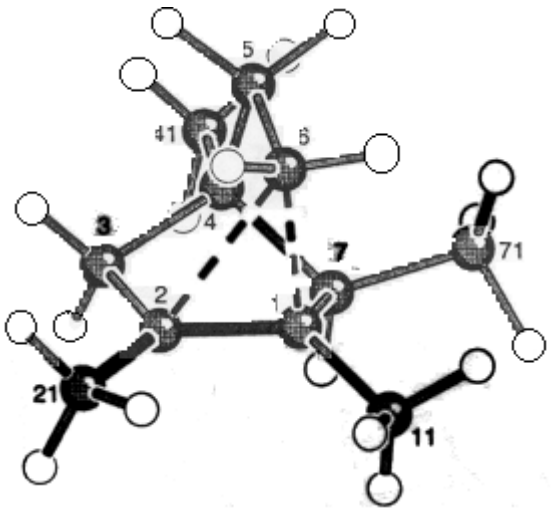

Figure 11 : Crystal structure of **41**

C2–C1	1.409(9)	$C_{sp^2}-C_{sp^3}(C_{sp^3})_3$	1.522(1)
C2–C21	1.457(8)	$C_{sp^2}-CH_3$	1.503(1)
C1–C11	1.503(8)	$(C_{sp^3})_3C_{sp^3}-CH_3$	1.534(1)
C2–C3	1.491(8)	$C_{sp^2}-CH_2(C_{sp^3})$	1.502(1)
C1–C6	1.710(8)	$(C_{sp^3})_3C_{sp^3}-CH_2(C_{sp^3})$	1.538(1)

Table 6 : Average structural parameters of **41** and corresponding reference parameters (in Å)

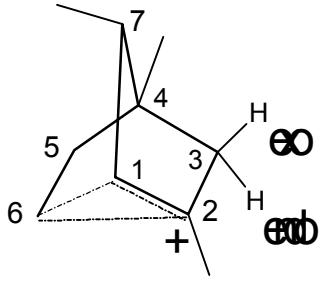

41

Scheme 29

geometry distorts significantly from that of a neutral norbornane. The shortening of C1-C2 bond (by 0.113 Å), C2-C21 bond (by 0.046 Å) and C1-C11 bond (by 0.031 Å) are significant while that of C2-C3 bond (by 0.011 Å) is not.The elongation of C1-C6

bond (by 0.172 Å) is also remarkable. These structural features are attributed to the interaction of empty p orbital of C2 with the occupied orbitals in its vicinity. The alignment of C1-C6 bond (torsional angle between the symmetry axis of p_{C2} and C1-C6 bond is -7º) is ideal for such an interaction forming a 3c, 2e bond among C1, C2 and C6. The p orbital of C2 concomitantly interacts with C21 methyl group and C3-H_{exo} bond but not to the same extent due to poor overlap.

In studies of hyperconjugative effects of substituents incorporated into bridgehead cations, it is necessary to have a rigid structure which will not distort in such a way to include the effects like bridging. The latter kind of interference will obscure the effect of substituents.

4. Methods

For investigating hyperconjugative interactions in molecular systems, employment of electron correlation is necessary. A basic approximation of the Hartree-Fock scheme is the neglect of the local distortion of the distribution of electrons. Instead of an orbital being distorted in the vicinity of another electron, the whole orbital is modified in an averaged way. Therefore, the scheme neglects local electron-electron effects- it neglects electron correlations. An approach to handle electron correlation is included in Density Functional Theory (DFT) methods.[109] DFT methods compute electron correlation via general functionals of the electron density. DFT functionals partition the electronic energy into several components which are computed separately: kinetic energy, the electron- nuclear interaction, the Coulomb repulsion and an exchage-correlation term accounting for the remainder of the electron- electron interaction (which is divided into separate exchange and correlation components in most actual DFT formulations). Another approach to electron correlation is Moller-Plesset perturbation theory. Qualitatively, Moller-Plesset perturbation theory[110] adds higher excitations to Hartree-Fock theory as a non-iterative correction, drawing upon techniques from the many-body perturbation theory. In this study, both approaches are included by employing MP2 (a 2nd order Moller-Plesset perturbation theory method) and B3LYP (a Density Functional Theory method which employs Lee-Yang-Parr correlation functionals, combined with the Becke three parameter hybrid exchage functional) levels of theory both of which include electron correlation are used in handling the molecular systems.

The basis sets, 6-31+G (2d) and 6-31+G*, are among the commonly used ones for similar computational studies. The polarization functions in these basis sets give the orbitals the flexibility to change their shape. The diffuse functions are included due to their necessity to handle molecules having electrons relatively far from the nucleus (e.g. molecules with lone pairs, anions).

All the stationary points included in parts 5 and 7 have been confirmed by frequency calculations: the ground state structures have no imaginary frequencies and the transition structures have only one imaginary frequency.

Gaussian 98 program suite[101] with its WINDOWS and LINUX versions is used to perform all the computations. Natural Bonding Orbital (NBO) analysis[102] which is implemented in the Gaussian 98 is used to analyze the electron distribution of the molecules. The NBO analysis transforms the canonical delocalized Hartree-Fock MOs into localized orbitals that "are closely tied to chemical bonding concepts". This process involves sequential

transformation of nonorthogonal atomic orbitals (AOs) to the sets of "natural" atomic orbitals (NAOs), hybrid orbitals (NHOs) and bond orbitals (NBOs). Each of these localized basis sets is complete and orthonormal. Importantly, these sets also describe the wavefunction in the most "economic" way since electron density and other properties are described by the minimal amount of field orbitals in the most rapidly convergent fashion. Filled NBOs describe the hypothetical, strictly localized Lewis structure. The interactions between filled and antibonding (or Rydberg) orbitals represent the deviation of the molecule from the Lewis structure and can be used as a measure of delocalizations. Since the occupancies of filled NBOs are highly condensed, the delocalizing interactions can be treated by a standard 2^{nd}-order perturbation approach or by deletion of the corresponding off-diagonal elements of the Fock matrix in the NBO basis. Thus, the NBO method which treats the molecule in terms of localized electron-pair "bonding" units is often used to investigate hyperconjugation as reflected in 2^{nd} order perturbation energies and NBO occupancies.

For visualization purposes, the MOLEKEL[103] and MOLDEN[104] program packages are used. Linear and multiple regression analysis and sketching of the plots are employed by Origin 6.0 and Microsoft Excel programs.

5. N/π Resonance Interactions of the Amide Linkage:

N,N- Dihaloformamides, -thioformamides and –selenoformamides

5.1.Results

All the amides investigated in this part are defined in Scheme 30. The conformers (ground state (GS) structure, rotational transition (RT) structure and inversion transition (IT) structure) of these molecules are shown in Figure 12.

	X	Y
42	O	H
43	S	H
44	Se	H
45	O	F
46	S	F
47	Se	F
48	O	CH_3
49	S	CH_3
50	Se	CH_3

	X	Y
51	O	Cl
52	S	Cl
53	Se	Cl
54	O	Br
55	S	Br
56	Se	Br

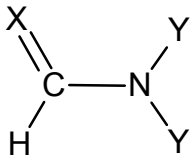

Scheme 30

5.1.1. Molecular Geometry

Among the geometry parameters, the most important ones are C-N and C=X bond lengths and the pyramidalization of the amide N (where X is O, S or Se). These values (only the MP2/ 6-31+G (2d) results) are listed in Table 7.

(a) (b) (c)

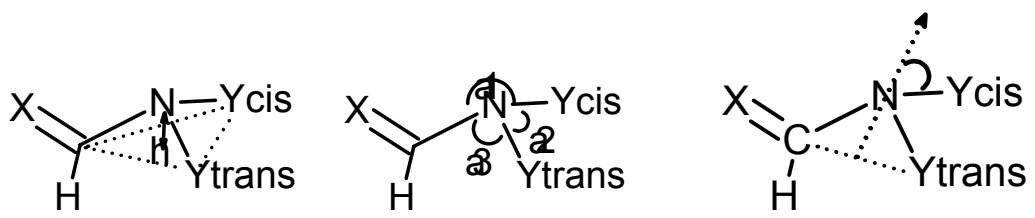

Scheme 31

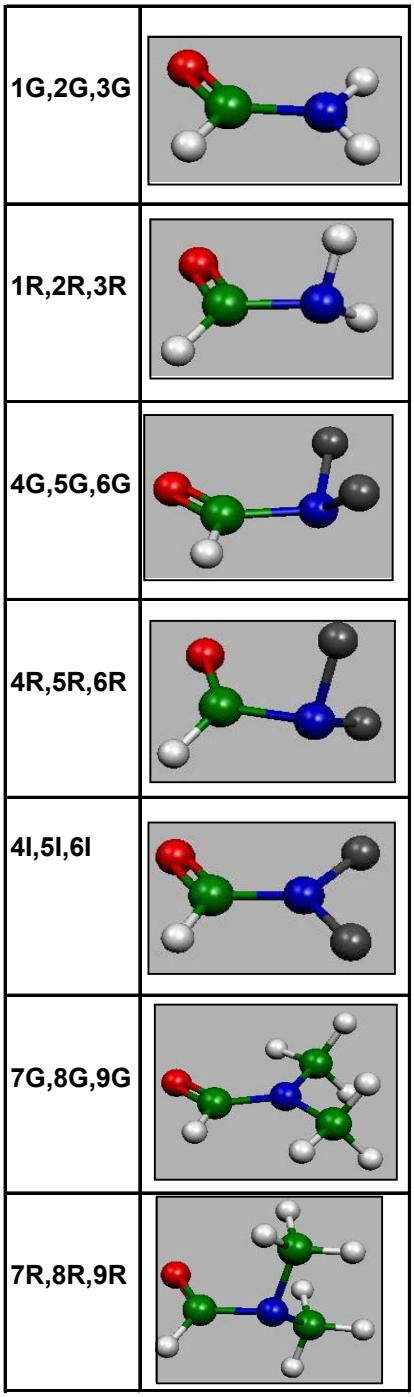

Figure 12: Examples of conformers of the molecules in Scheme 30.
G: ground state structure, R: rotational transition structure, I: inversion transition structure. Numbers 1-9 correspond to structures **42-50**.

There are three basic ways to measure the magnitude of pyramidalization:

(1) Finding the distance of N atom to the plane formed by Y_{trans}-C-Y_{cis}: Scheme 31 (a)

(2) Finding the sum of angles a1, a2 and a3 around N: Scheme 31 (b)

(3) Finding the supplementary angle of Y_{trans}-N-C-Y_{cis} dihedral angle. Scheme 31 (c)

In this part, the pyramidalization values are defined to be the supplementary angle of the Y_{trans}-N-C-Y_{cis} dihedral angle.

The unsubstituted amides **42-43** and N,N-dimethyl amides **48-50** are nearly, if not exactly, planar in the ground state (GS) structures (Table 7). However, the GS structures of N,N-difluoro amides **45G**, **46G**, and **47G** are found to be highly pyramidalized. Their pyramidalization is even larger than those of the RT conformers of unsubstituted amides and thus, they are close to tetrahedral structures. It is comparable with the pyramidalization of NH_2F which is 76.1˚.

The C-N and C=X bond lengths have a large range throughout the series. For all unsubstituted and N,N-dimethyl amides, the C-N bonds of the GS structures (**42G-44G** and **48G-50G**) are considerably shorter compared to their rotational transition (RT) structures

Structure No	C-N bond length	C=X bond length	Pyramidalization
42G	1.3599	1.2208	0
42R	1.444	1.2111	69.3
43G	1.3468	1.6409	0
43R	1.4397	1.6237	68.3
44G	1.3431	1.7685	0
44R	1.4368	1.7517	67.4
45G	1.4722	1.196	70.7
45R	1.5207	1.1924	73.9
45I	1.3699	1.2111	0
46G	1.4378	1.6095	70.1
46R	1.4865	1.6067	73.5
46I	1.339	1.6351	0
47G	1.426	1.739	69.9
47R	1.4707	1.7385	73.7
47I	1.3303	1.7637	0
48G	1.36	1.2264	0.2
48R	1.4407	1.2125	58.7
49G	1.3416	1.6532	0
49R	1.4335	1.6279	56.5
50G	1.336	1.7793	0
50R	1.4266	1.3303	56

Table 7: The geometry parameters of amides (MP2/ 6-31+G (2d) results). Bond lengths are in Å. Pyramidalization (in degrees) is found by taking the supplementary angle of Y_{trans}-N-C-Y_{cis} dihedral angle as shown in Scheme 31.

(**42R-44R** and **48R-50R**). In a similar fashion, the C=X bonds of the GS structures (**42G-44G** and **48G-50G**) are longer than those of RT structures (**42R-44R** and **48R-50R**) but the difference is only in the order of 0.01 Å.

Among the N,N-dihalo amides the N,N-difluoro amides display the largest effects of substitution on molecular geometry. The C-N bond is the shortest in the inversion transition (IT) structures (**45I-47I**) and then follow the GS structures (**45G-47G**) and the RT structures (**45R-47R**), respectively. The C=X bond length increases in the reverse order: RT structure, GS structure, IT structure, respectively. But the change in the C=X bond length is much smaller than that of the C-N bond, as in the previous case.

Additionally, among the same conformers of amides which differ only in heteroatoms (e.g. **42G**, **43G**, **44G** or **45R**, **46R**, **47R**) , the C-N bond is shortening while the heteroatom changes from O to S to Se, respectively.

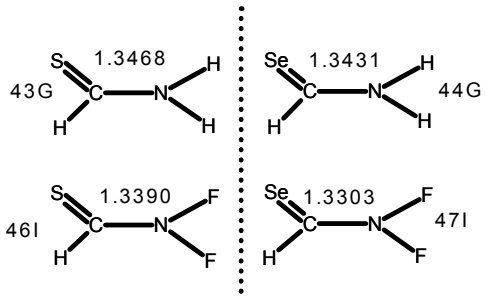

Scheme 32

The comparison of C-N bond of **46I** with that of **43G** and **47I** with that of **44G** yields an interesting result (Scheme 32). The C-N bonds of **46I** and **47I** are shorter than those of **43G** and **44G**, respectively. Having the same connectivity and conformation, the only difference between them is replacement of H atoms by F atoms. A similar comparison of the RT conformers gives an opposite result (Scheme 33): the C-N bonds are elongated while

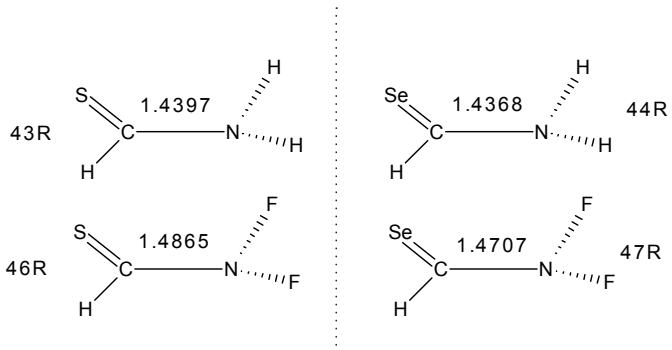

Scheme 33

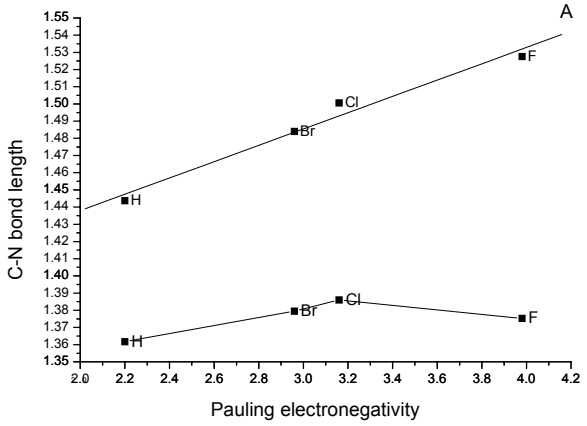

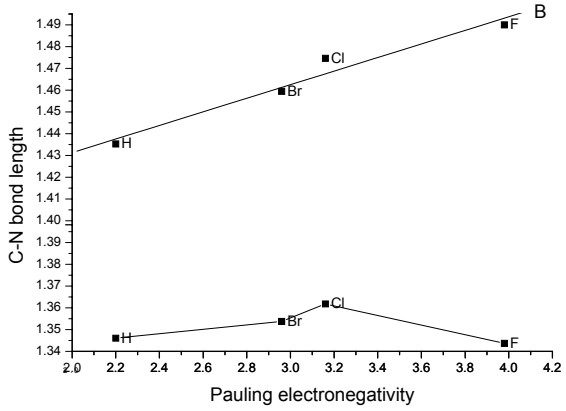

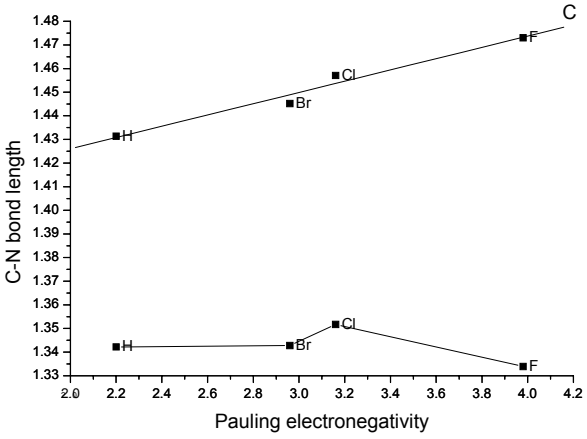

Figure 13: C-N bond lengths (in Å) of dihalogenated oxo-, thio- and seleno-formamides The upper line corresponds to RT conformers and the lower line to all-planar conformers. A: oxoamides B: thioamides C: selenoamides (B3LYP/6-31+G* results)

going from unsubstituted **43R** and **44R** to N, N-difluoro substituted **46R** and **47R**, respectively.

N, N-difluoro amides show a discrepancy also among the series of N, N-dihalo amides. N, N-difluoro amides remain highly pyramidalized in the chalcogen replacement series while the pyramidalization of N, N-dichloro amides decreases significantly on going to heavier chalcogens (Table 8). In the RT conformers the C-N bond lengthens with increasing electronegativity of the substituent (Figure 13). However, the all-planar conformers indicate a distinct drop from the monotonic line for N, N-difluoro amides. The N-halogen bond lengths for N, N-difluoro amides are also remarkably shorter than those of the heavier halogens (Figure 14)

No	θ_N
45	68.7
46	66.9
47	66.4
51	37.3
52	17.4
53	0.1
54	0
55	0
56	0

Table 8: Pyramidalization of N,N-dihalo amides (B3LYP/6-31+G* results) (in degrees)

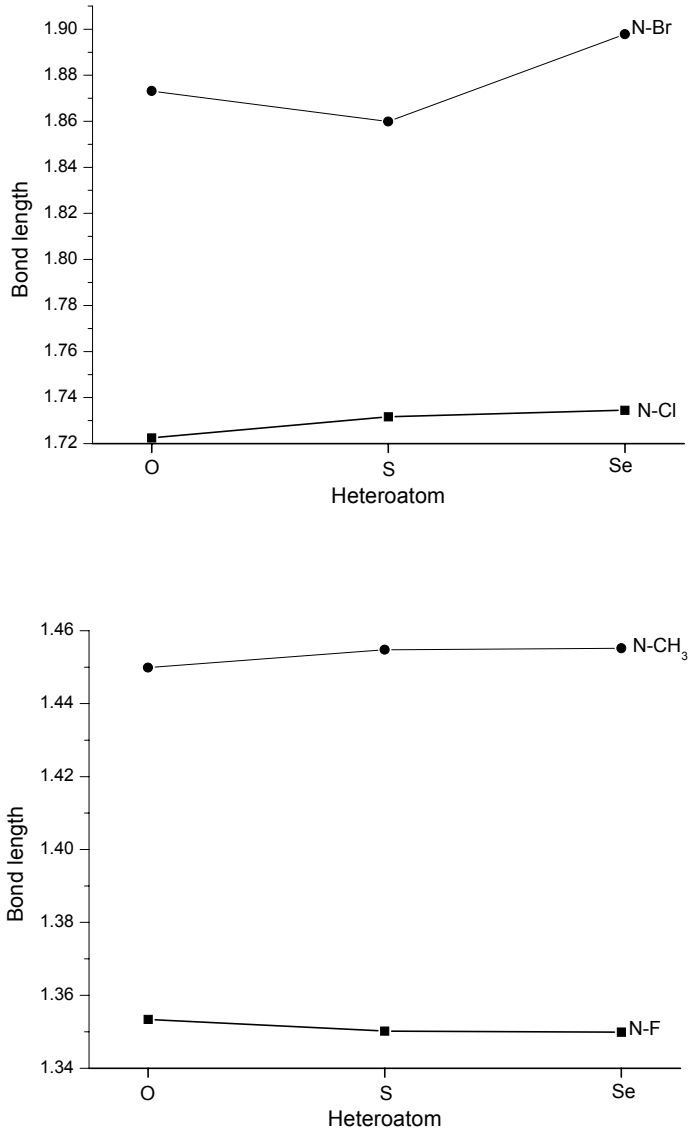

Figure 14: The N-halogen bond lengths with different heteroatoms in the planar IT structures (B3LYP/6-31+G* results) (bond lengths in Å)

5.1.2. Rotational and Inversion Barriers

Table 9 shows the rotational barriers for molecules **42**-**50**. The rotational barriers of N,N-dimethyl amides **48**-**50** are the largest and the unsubstituted amides **42**-**44** follow them. However, the values for N,N-difluoro amides **45**-**47** are significantly lower than all these. Also, unlike the others, N,N-difluoro amides do not have the increasing trend in rotational barriers while going from oxoamides to selenoamides.

Table 9 also contains the inversion barriers for N,N-difluoro amides **45**-**47**.It is observed that the inversion barrier decreases as one proceeds in the series from **45** to **47**.

Structure No	Rotational barrier	Inversion barrier
42	16.29	
43	18.88	
44	19.41	
45	5.51	15.74
46	5.56	14.3
47	5.24	13.81
48	19.46	
49	22.39	
50	23.86	

Table 9: Rotational and inversion barriers for amides in kcal/mol
(MP2/6-31+G (2d) results. ZPE corrections included.)

5.1.3. Group-Transfer Energies

Group-transfer energies are obtained as heats of the isodesmic reactions shown in Schemes 34-39. An isodesmic reaction is a reaction in which both the reactants and the products have the same number of bonds of a given type but there may be changes in the relationship of one bond to another.[105] All the group-transfer energies (GTE) are obtained using MP2/6-31+G (2d) energies with ZPE corrections included.

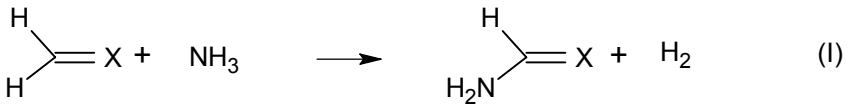

(I)

X	No	GTE (kcal/mol)
O	**42G**	-9.83
O	**42R**	6.45
S	**43G**	-6.39
S	**43R**	12.49
Se	**44G**	-6.97
Se	**44R**	12.45

Scheme 34

GTE values for reaction (I) reflect the strength of interaction of NH_2 moiety with the rest of the amide (Scheme 34). The reaction is exothermic for GS structures but endothermic for the RT structures.

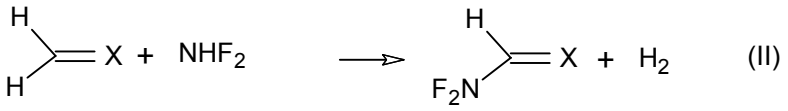

X	No	GTE (kcal/mol)
O	**45G**	2.27
O	**45R**	7.78
O	**45I**	18.01
S	**46G**	4.42
S	**46R**	9.98
S	**46I**	18.72
Se	**47G**	2.06
Se	**47R**	7.29
Se	**47I**	15.87

Scheme 35

GTE values for reaction (II) reflect the strength of interaction between NF_2 moiety and the carbonyl group of the amide for N, N-difluoro amides. The plot of these GTE values versus the percentage p character of the N *lp* of the amide does not reveal a monotonic linear correlation but rather shows a drop and a rise, respectively (Figure 15). It is also worth to note that the relative GTE values for chalcogens do not follow directly the order of them in the periodic table.

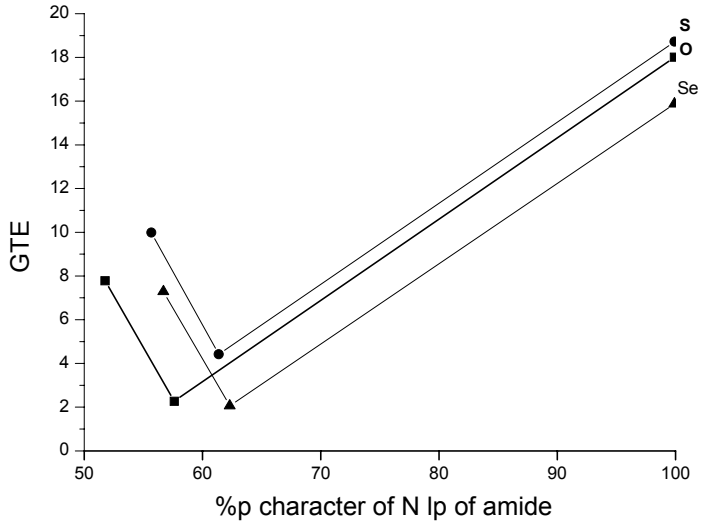

Figure 15: Correlation between GTE values of reaction (II) for conformers of **45-47** vs. p character percentage of N *lp* of the amide

GTE values of reactions IV, V and VI for different conformations of N,N-difluoro amides **45-47** and N,N-dimethyl amides **48-50** have been listed in Schemes 37, 38 and 39. These reactions show the effect of incorporation of the N-substituents (F or CH_3) into the molecule. To make a comparison, the corresponding GTE values for NH_3 are also included (Scheme 36).

$$NH_3 + HF \longrightarrow NH_2F + H_2 \qquad \text{GTE= 69. 65 kcal/mol} \qquad \text{(III)}$$

$$NH_3 + CH_3F \longrightarrow NH_2F + CH_4 \qquad \text{GTE= 44. 16 kcal/mol} \qquad \text{(IV)}$$

Scheme 36

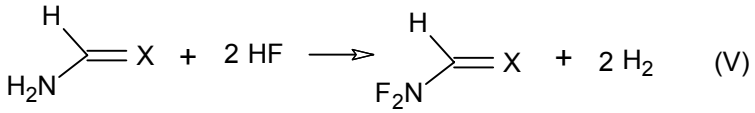

X	No	GTE(kcal/ mol)
O	**45G**	133.54
O	**45R**	127.89
O	**45I**	154.41
S	**46G**	131.28
S	**46R**	124.05
S	**46I**	151.67
Se	**47G**	129.17
Se	**47R**	121.41
Se	**47I**	149.40

Scheme 37

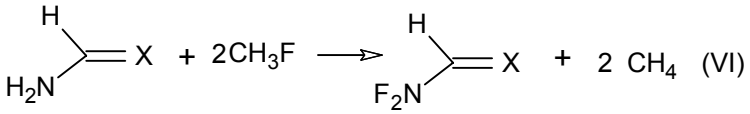

X	No	GTE(kcal/ mol)
O	**45G**	82.56
O	**45R**	76.97
O	**45I**	103.49
S	**46G**	80.36
S	**46R**	73.13
S	**46I**	100.75
Se	**47G**	78.25
Se	**47R**	70.49
Se	**47I**	98.47

Scheme 38

While obtaining GTE for reactions V, VI and VII, it is given special importance to include unsubstituted and N, N-disubstituted amides having the same or at least similar conformations. In this way, it is aimed to exclude energetic effects of conformation changes and to see the effect of substitution solely. In terms of conformation, RT structure of N, N-

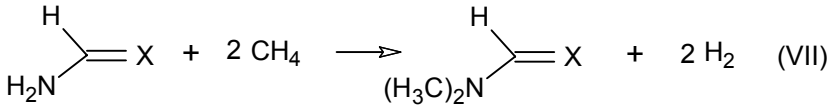

X	No	GTE
O	**48G**	30.62
O	**48R**	33.80
S	**49G**	28.11
S	**49R**	31.62
Se	**50G**	24.79
Se	**50R**	29.23

Scheme 39

difluoroformamide **45R** corresponds to the RT structure of formamide **42R** and the IT structure of N,N-difluoroformamide **45I** corresponds to GS structure of formamide **42G**. To correspond to the GS structure of N,N-difluoroformamide **45G**, an additional formamide structure has been optimized with the angles around N constrained to those of **45G**. The same procedure has been applied for S and Se analogues.

For N,N-difluoro amides, **45**-**47**, two different reactions (V and VI) are used separately to obtain GTE and they both give the same trend. Among the three conformers of the same N,N-difluoro amide, the reaction of the RT structure is the least endothermic and that of the IT structure is the most endothermic.

Comparison of the GTE values for each conformer of N,N-difluoroformamide **45** with the corresponding conformers of thio- and seleno- analogues (**46** and **47**) show that GTE are largest for oxoamides **45** and decrease in the chalcogen (S, Se) series (Scheme 37 and 38).

The correlation between GTE and hybridization of N lone pair is presented in Figure 16. In addition to the three conformers of for each N,N-difluoro amide, two other structures with constrained pyramidalization values have been optimized and included for **45** and **48**. The plot indicates a direct proportionality between GTE and p character percentage of N *lp*.

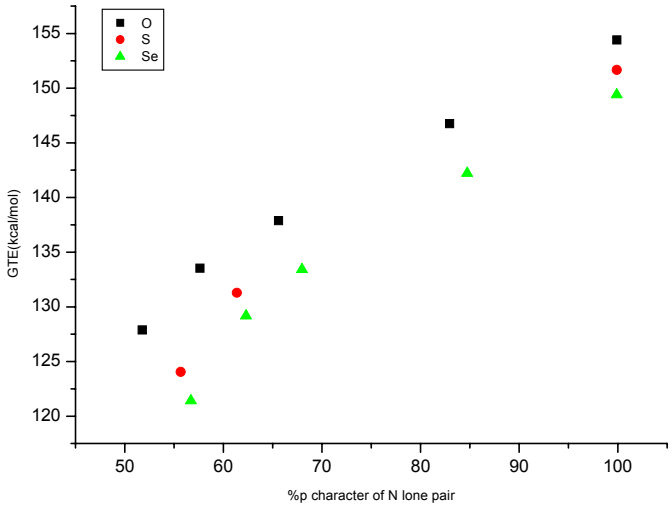

Figure 16: Correlation between GTE and p character percentage of N lone pair

5.1.4. Electronic Structure

5.1.4.1. Formamide as a Three-Center 2p Orbital (Allyl-like) system

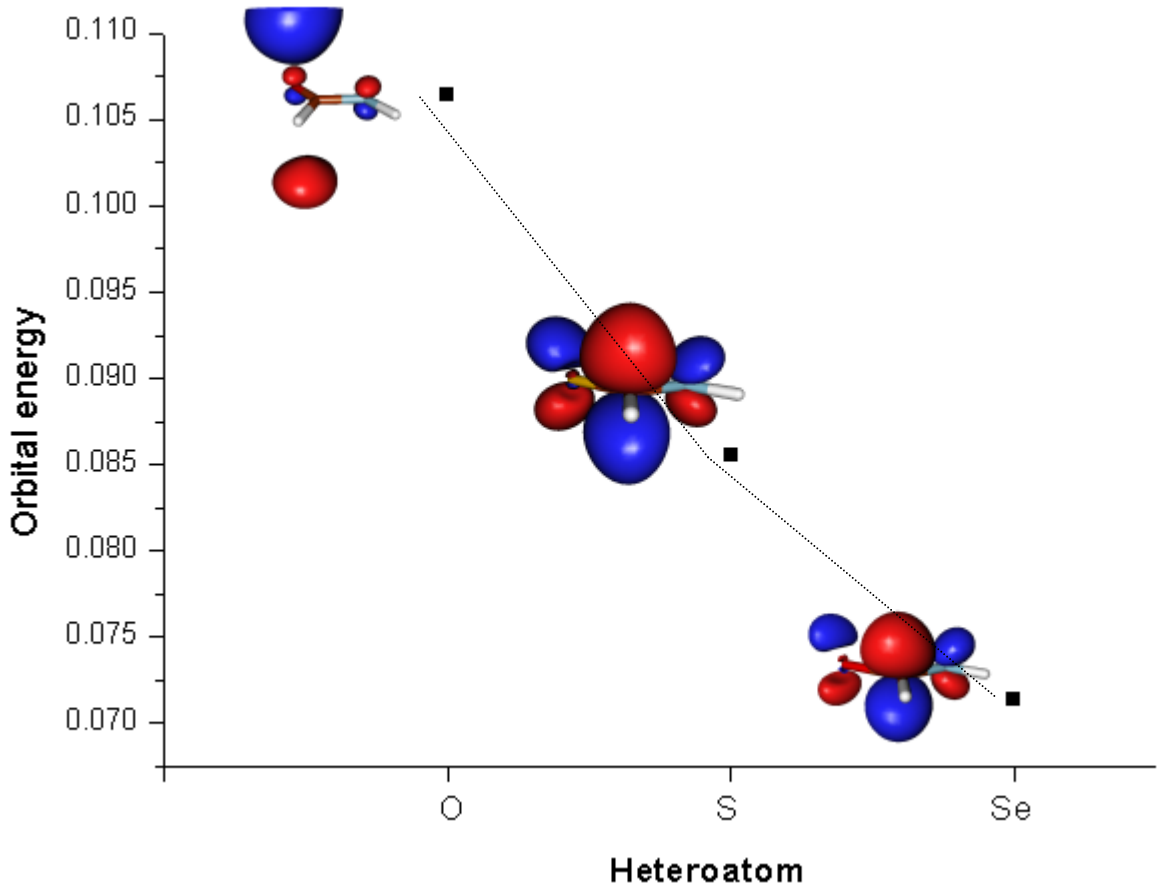

Figure 17: The energies(in Hartrees) of π-like unoccupied MOs of IT structures of **42-44**

The analysis of molecular orbitals of IT structures of unsubstituted amides reveal that one of the unoccupied orbitals of the amide linkage is just like that of an allyl group with a p orbital system of three centers (Figure 17). This molecular orbital is the one which would interact in π-fashion with the incoming π –donor substituents. The plot shows that the energy of this antibonding orbital decreases as one goes from oxo- to seleno- amides which means selenoamides will be the best acceptor among them for any incoming π–donor substituent. The extensions of the molecular orbitals also change with different heteroatoms.

5.1.4.2. π- Symmetry MOs of the N,N- Difluoroformamide IT Structure

It is of great interest whether F atoms contribute to the amide resonance in π –fashion with their lone pairs despite its high electronegativity. The analysis of occupied molecular orbitals (MOs) shows that there are 4 different π–type MOs which are exhibited in Figure 18. The lowest energy orbital shows π–bonding between N and F atoms. The energy of this orbital decreases on going from O to Se.

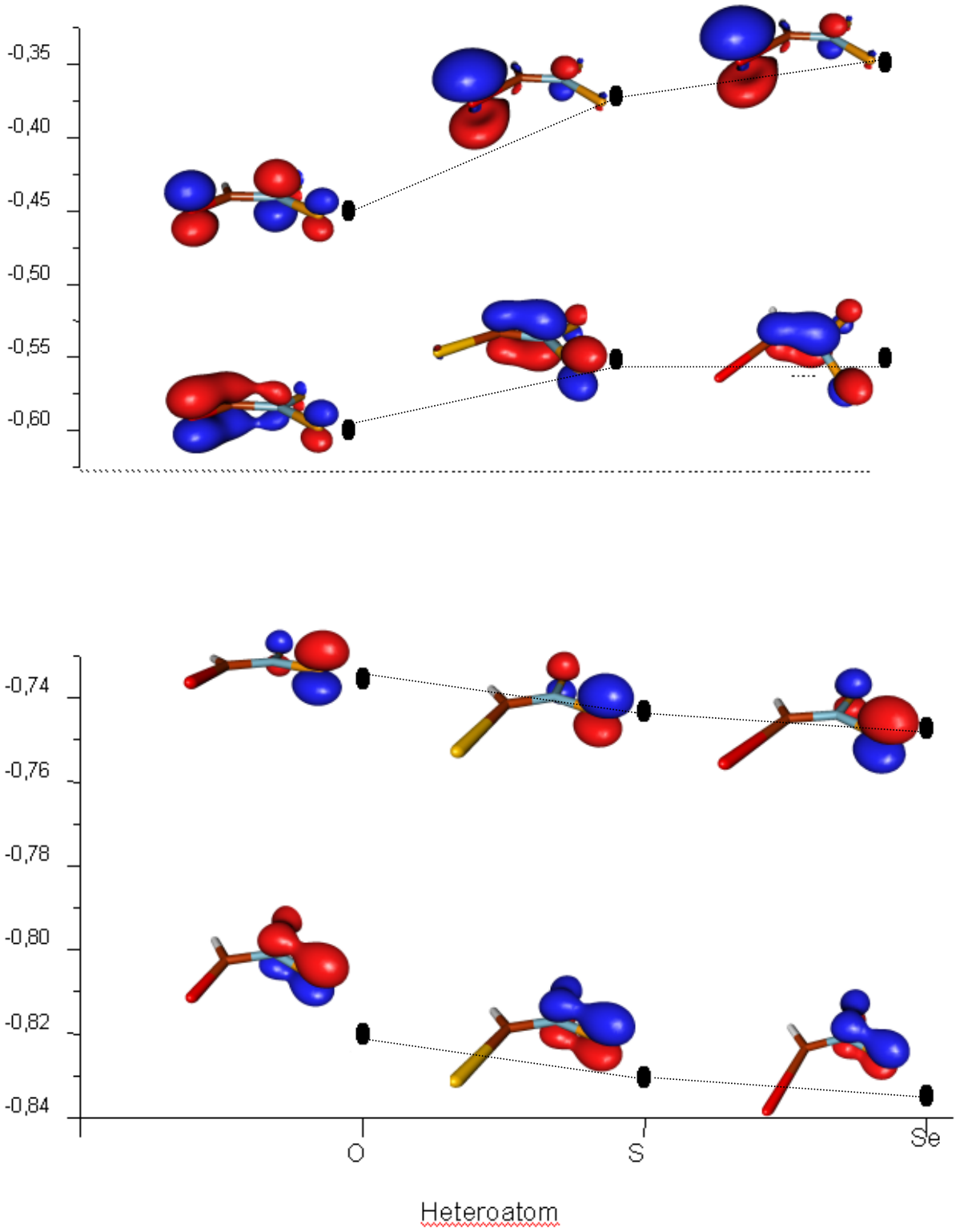

Figure 18: The energies (in Hartrees) of π –type occupied MOs of **45-47**

5.1.5. Electron Density Distribution

5.1.5.1. AIM Bond Orders

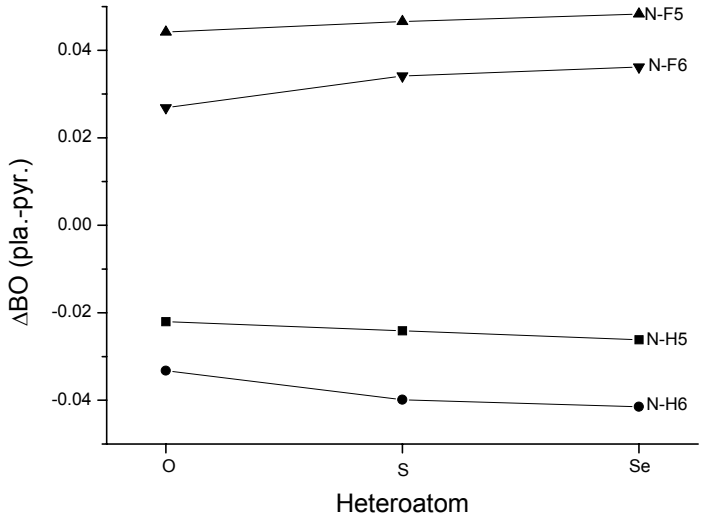

Figure 19: AIM bond order changes of N-H bonds of amides and N-F bonds of N,N -difluoro amides while going from pyramidal conformer to planar conformer

The trend of AIM bond order changes while going from nonplanar conformers to planar conformers are different for N-H bonds of unsubstituted amides and N-F bonds of N,N-difluoro amides (Figure 19). Going to the planar structure causes reduction of N-H bond orders while it causes an increase of N-F bond orders. The changes in the bond orders are larger for heavier chalcogens (Figures 19 and 20).

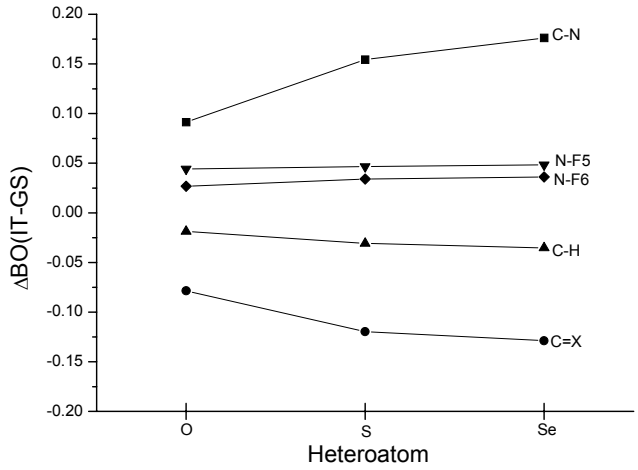

Figure 20: AIM bond order change of N,N-difluoro amides while going from GS to IT structure

5.1.5.2. NBO Results for Fluorine Atoms of N, N-Difluoro Amides

The NPA atomic charges for F atoms are presented in Table 10. According to the table, for each N,N-difluoro amide the F atoms of GS and RT conformers have similar

Structure No	F_{trans}	F_{cis}
45G	-0.27533	-0.24597
45R	-0.26981	-0.2698
45I	-0.20278	-0.18966
46G	-0.27271	-0.2463
46R	-0.27154	-0.27161
46I	-0.19624	-0.17856
47G	-0.27135	-0.24698
47R	-0.2727	-0.2727
47I	-0.194	-0.1756

Table 10: NBO atomic charges for F atoms of N, N-difluoro amides.
Cis and *trans* positions are with respect to heteroatom of C=X bond.

amounts of electron density while the F atoms of IT conformers differ from them with a much lower electron density.

	45--->46	**45--->47**
LP(1)F5	0.0006	0.0008
LP(2)F5	0.0024	0.0033
LP(3)F5	-0.0009	-0.0010
LP(1)F6	0.0000	-0.0002
LP(2)F6	0.0036	0.0047
LP(3)F6	0.0000	0.0000

Table 11: The change in Δe[GS-IT] on going from **45** to **46** and from **45** to **47**

When the NBO occupancies of *lp*s of F atoms are investigated, it is observed that the occupancy of LP(2) decreases on going from GS to IT structure (Δe[GS-IT]). Moreover, a remarkable change occurs in Δe[GS-IT] of LP(2) on going from **45** to **46** and from **45** to **47** while it is almost constant for the other *lp*s, as seen in Table 11 . The pictures of *lp*s of F atoms in Figure 21 show that LP(2) electrons are the ones lying in the π-frame. The hybridization of these *lp*s are listed in Table 12.

Orbital	% s	% p	Orbital	% s	% p
5G LP1 (F5)	51.95	48.01	**5I** LP1 (F5)	81.97	18.01
5G LP2 (F5)	32.44	67.52	**5I** LP2 (F5)	0.00	99.93
5G LP3 (F5)	1.42	98.51	**5I** LP3 (F5)	2.18	97.73

Table 12: The hybridization of *lp*s of F atoms of N, N-difluorothioformamide (corresponding to those shown in Figure 21)

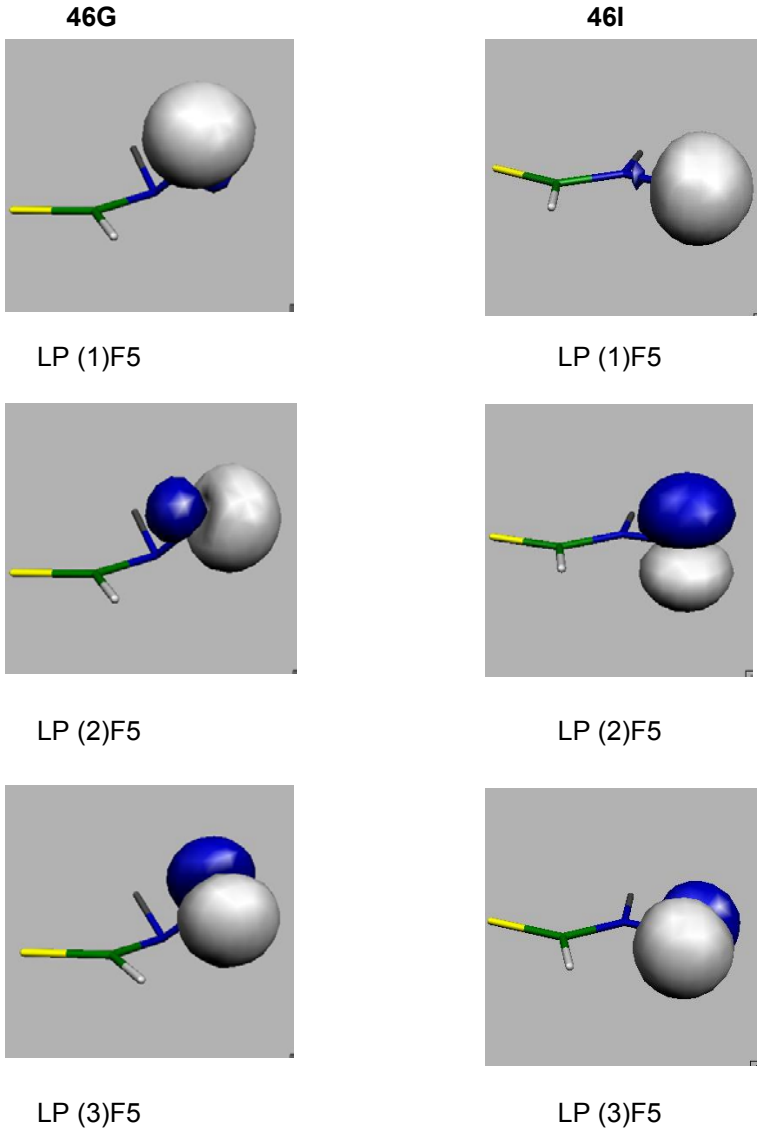

Figure21: NBO orbitals of F *lp*s of N, N-difluorothioformamide

5.2. Discussion

The effect of N-halo substitution on the potential energy surface of formamide is found to be generally related to electronegativity of halogens. Thus, N, N-difluoroformamide is highly pyramidalized in the ground state, and the all-planar form becomes now the transition structure for inversion. The N pyramidalization is consistent with the Bent's rule[108] which states that the electronegative substituent calls for increase in the *p* character in the bond forming orbital of N, increasing the *s* character of the orbital occupied by the unshared electron pair. Fluorinated N remains highly pyramidalized in the entire O, S, Se series (θ_N = 68.7º, 66.9º, and 66.4º at B3LYP/6-31+G*). In contrast, pyramidalization is smaller in N, N-dichloroformamide and decreases in the chalcogen substitution series (θ_N = 37.3º, 17.4º, and 0.1º at B3LYP/6-31+G*), which reflects increasingly successful competition of π-bonding stabilization of the planar form in the case of heavier chalcogens. The trend of increase in π-bonding across the C-N bond, reflected in the increase in barrier to rotation in the formamide chalcogen-substitution series, is preserved in N-halo derivatives, although in the case of N, N-difluoro amides it is manifested in the magnitude of the inversion barriers rather than of the rotational barriers (Section 5.1.2 , Table 9). Finally, pyramidalization does not occur at all in the N, N-dibromo amides due to the lower electronegativity of Br.

The effect of electronegativity is also expected to be shown in variation of bond distances. Indeed, for instance the C-N bond distances in the transition structures for rotation, where there is relatively little π-bonding, correlate quite well with Pauling electronegativities (Section 5.1, Figure 13).

The striking exception to this general trend is found, however, upon the attempt to correlate in the same way the C-N bond distances in all-planar conformers (equivalent to transition structures for inversion in the case of F and Cl substitution, equivalent to ground state structures in the case of Br), with the full extent of π-bonding. Here, fluorine substitution causes considerable shortening of the C-N bond rather than the expected elongation, and the effect is increasing in the chalcogen-substitution series, so that the C-N bonds in the N, N-difluoro amides actually become shorter in these all-planar conformers than those in the parent unsubstituted amides (Section 5.1.1, Figure 13, Schemes 32, 33).

This anomaly suggests that the F atom is in fact capable of stabilizing the polar resonance form of the amide linkage by π-donation. This implies in turn that the N-F bond would be strengthened by π-bonding. There is some evidence to support this contention. In the chalcogen-substitution series, X=O, S, Se, the N-Y bond distances in all-planar conformers increase when Y=H, CH_3, Cl, Br, but do decrease when Y=F (Section 5.1.1, Figure 14). The AIM N-F bond orders change in the consistent manner (Section 5.1.5.1, Figures19, 20). In the transition structures for inversion of N, N-difluoro amides, the lowest energy occupied π-symmetry orbital extends over N-F in the in-phase combination, and its energy is lowered in the series X=O, S, Se (Section 5.1.4.2, Figure 18). On going from the ground state to the inversion transition structure, electron density shift from the F atoms occurs (Section 5.1.5.2, Table 10). Comparison of the occupancy of the localized NBO orbitals in N, N-difluoroamides in the series X=O, S, Se, indicates that as far as the nonbonding electron density is concerned, the chalcogen effect (the loss of charge) is manifested mostly in the $2p_z$ F *lp* (Section 5.1.5.2, Table 11, Figure 21), the one that interacts with the π-system of the amide linkage.

However, examination of the heats of isodesmic reactions of substitution at the amide N did not show any significant effects in terms of bond energies. The group-transfer energies from the reactions of amide formation reflect both electronegativity and π-bonding influences. The group-transfer reaction of rotational transition structure for formamide is endothermic because of electronegativity, but that of the ground state formation is exothermic, electronegativity being offset by π-bonding; for N, N-difluoro amides, overall trend dicated by increase in electronegativity, but endothermicity is strongly affected by π-bonding for the ground state. On the other hand, for N substitution, only electronegativity effect is observed, anything else is small if present.

6. N/σ Resonance Interactions of the Amide Linkage: 2,3-Disubstituted N-Acyl-7-azabicyclo(2.2.1)heptanes

6.1. Results

6.1.1. Molecular Geometry

6.1.1.1. N-Acetyl-7-azabicyclo(2.2.1)heptanes

The parent structure **57** and its 2,3-*endo,endo*-disubstituted derivatives **58-66** have been optimized using the B3LYP/6-31+G(2d) level of theory. In the optimized molecule, the

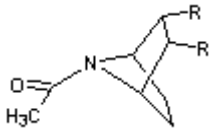

57-66

Scheme 40

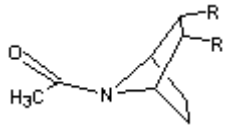

67-74

		R
57	:	H
58, 67	:	F
59, 68	:	Cl
60, 69	:	CH_3
61, 70	:	CF_3
62, 71	:	CN
63	:	-NH-CH_2-HN- =RR
64, 72	:	N=PH_3 (P-N-C7-C5 and P-N-C8-C6 dihedral angles constrained to 90˚)
65	:	N=PH_3 (P-N-C7-C5 and P-N-C8-C6 dihedral angles constrained to 180˚)
66, **73**	:	$CHCH_2$
74	:	COOH (C5-C7-C-O dihedral angles constrained)

amide nitrogen, which is usually coplanar, has been found to be pyramidalized significantly. There are three basic ways to measure the pyramidalization (Figure 22):

1. Summing up the three angles around N, which will make 360˚ in a coplanar structure.
2. Finding the distance of N atom to the plane formed by C2, C6 and C5. (see Figure 22 for numbering)
3. Finding the torsional angle of C5-N-C6-C2 which will range from -180˚ to +180˚.(see Figure 22 for numbering)

(a) (b)

Figure 22: Visualization of (a) *syn*- and (b) *anti*- pyramidalization

In our study, we use the third definition but take the supplementary angle of the dihedral angle of C5-N-C6-C2. Thus, this angle θ represents how many degrees C5 should be moved to be in the plane formed by C6, N and C2 (Figure 22). (+) and (-) angles represent clockwise and counterclockwise directions. For convention, *syn*-pyramidalization will represent (+) torsional angles and *anti*-pyramidalization will represent (-) dihedral angles throughout the text.

Using this convention, the optimized parent structure **57** is found to have a pyramidalization of 31.1˚. The structures **58**-**66** with substituents of different electronic properties make only small changes in the pyramidalization compared to that of parent

Structure No	Pyramidalization
57	31,1
58	28,9
59	28,8
60	30,7
61	33,6
62	31,7
63	29,5
64	26,4
65	28,0
66	30,0
67	-24,6
68	-29,5
69	-31,2
70	-33,7
71	-33,9
72	-27,8
73	-31,6
74	-32,8

Table 13: Pyramidalization values of structures **57**-**74** (in degrees)

structure **57** (Table 13). Their pyramidalizations range from 26.4˚ to 33.6˚. Thus, the effect of remote substitution is rather small compared to the dominant effects causing the pyramidalization of the parent structure.

The *anti*-pyramidalized structures have very similar energies to their *syn*-pyramidalized analogues (Table 14). The differences are in the order of 0.001 Hartrees or less.

No	Energy(*syn*)	No	Energy(*anti*)
57	-442.6799		-
58	-641.1659	**67**	-641.1655
59	-1361.8668	**68**	-1361.8672
60	-521.3044	**69**	-521.3044
61	-1116.8086	**70**	-1116.8088
62	-627.1608	**71**	-627.1616
63	-591.4744		-
64	-1237.1875		-1237.1878
65	-1237.1810		-
66	-597.4666	**73**	-597.4670
	-	**74**	-819.8365

Table 14: Comparison of energies of *syn*- and *anti*-pyramidalized structures (in Hartrees)

The inversion barriers have been determined for the parent structure **57** and one of the derivatives, **66**, by taking the energy difference between the fully-optimized structure and a structure in which N is constrained to be coplanar with the neighbouring C2, C5 and C6 atom. 0.31 kcal/ mol and 0.25 kcal/ mol are found for **57** and **66**, respectively.

6.1.1.2. N-Thioacetyl-7-azabicyclo(2.2.1)heptanes

The parent structure **75** and its 2, 3-*endo,endo*-disubstituted derivatives **76-87** have been optimized (Scheme 41). The parent structure **75** deviates from planarity around the amide N by just a few hundredths of a degree (Table 15). Thus, it is practically planar. The substituted derivatives **76-87** considerably differ from the parent structure **75**. Their pyramidalizations range from -24.7˚ to +5.7˚. The range of pyramidalization (30˚) is larger than that of N-acetyl-7-azabicyclo(2.2.1)heptanes.

The change in the direction of pyramidalization with different substituents is rather interesting. Large pyramidalization values are found for **77**, **79**, **80** and **84**, which have electron withdrawing substituents but also for **82** and **85**, which have electron donating substituents. The direction of pyramidalization is in every case the same: *anti.*

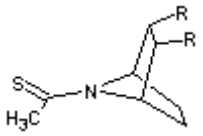

Scheme 41

R

75: H

76: F

77: Cl

78: CH_3

79: CF_3

80: CN

81: -NH-CH_2-NH-

82: N=PH_3 (P-N-C7-C5 and P-N-C8-C6 dihedral angles constrained to 90˚)

83: N=PH_3 (P-N-C7-C5 and P-N-C8-C6 dihedral angles constrained to 180˚)

84: COOH (C5-C7-C-O dihedral angles constrained)

85: $CHCH_2$

86: SiH_3

87: CCH

No	Pyramidalization
75	-0,1
76	5,7
77	-14,5
78	-4,9
79	-23,3
80	-24,7
81	0,2
82	-11,4
83	-7,1
84	-20,1
85	-14,0
86	-18,1
87	-16,4

Table 15: Pyramidalization values of structures **75-87** (in degrees)

The inversion barrier has been determined for one of the derivatives, **85**. It is found to be 0.06 kcal/mol, which is one order of magnitude smaller compared to the inversion barrier of the N-acetyl analogue of this structure (**66**).

6.1.1.3. 7-Bicyclo(2.2.1)heptyl Cations

The parent structure **88** and its 2,3-*endo,endo*-disubstituted derivatives **89-95** have been optimized (Scheme 42). As seen in Table 16, the parent structure is planar and the pyramidalization range of the derivatives lies from –18.3˚ to +17.8˚. Thus, 7-bicyclo(2.2.1) heptyl cations have the widest pyramidalization range among the three main structures investigated in this study.

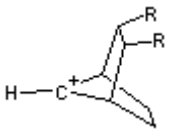

Scheme 42

	R
88:	H
89:	F
90:	Cl
91:	CH_3
92:	CF_3
93:	$CHCH_2$
94:	CCH
95:	COOH

No	Pyramidalization
88	0.0
89	16.9
90	16.8
91	-17.7
92	17.8
93	-18.3
94	-16.0
95	18.3

Table 16: Pyramidalization values for structures **88-95** (in degrees)

Net electron acceptor substituents induce *syn*-pyramidalization while net electron donor ones induce *anti*-pyramidalization.

6.1.2. NBO Analysis and Correlation Analysis of the Substituent Effects

6.1.2.1. Pyramidalization at C7 and N7 as a Function of Hyperconjugation

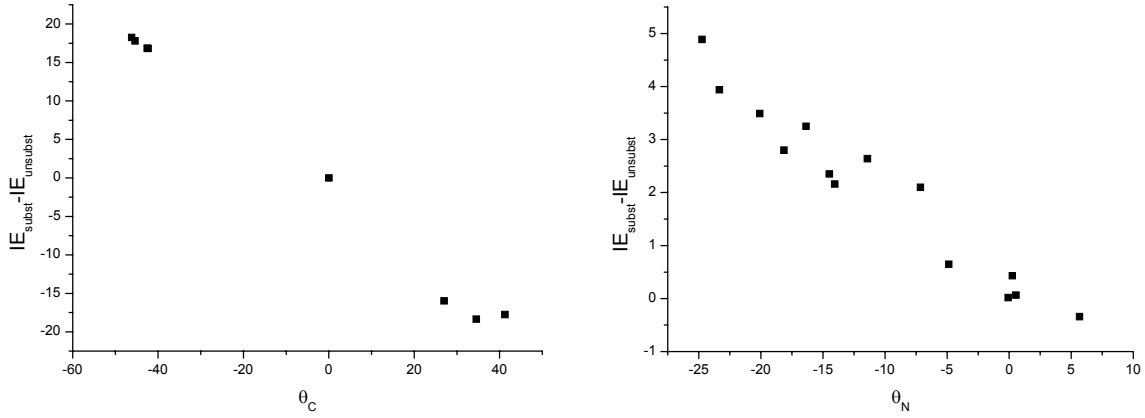

(A) (B)

Figure 23: The correlation between the pyramidalization (in degrees) and the difference of the interaction energies (in kcal/mol) of the N *lp* with the C-C bonds of substituted and unsubstituted bridges in (A) 2,3-*endo,endo*-disubstituted 7-aza-bicyclo(2.2.1) heptyl cations; (B) 2,3-*endo,endo*-disubstituted N-thioacetyl 7-azabicyclo(2.2.1)-heptanes.

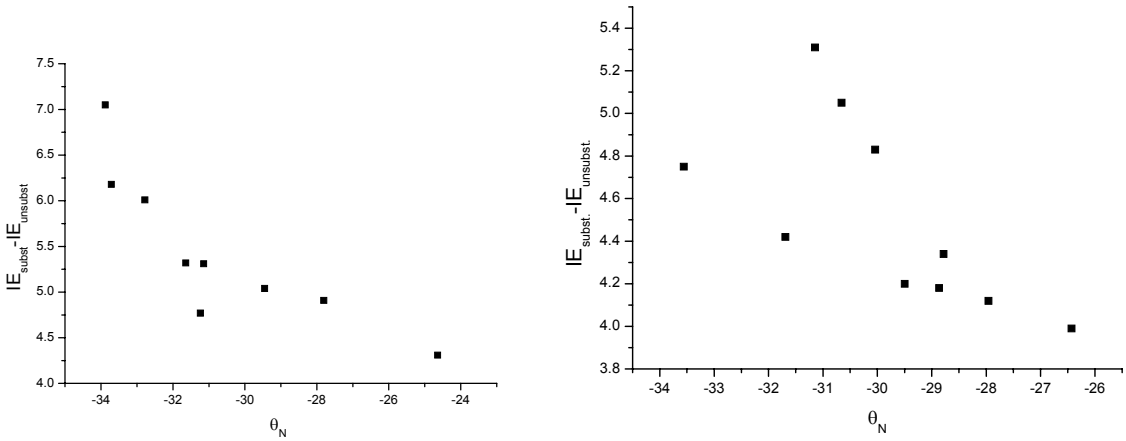

(A) (B)

Figure 24: The correlation between the pyramidalization (in degrees) and the difference of the interaction energies (in kcal/mol) of the N *lp* with the C-C bonds of substituted and unsubstituted bridges in (A) *anti*-pyramidalized 2,3-*endo,endo*-disubstituted N-acetyl 7-azabicyclo-(2.2.1)heptanes and (B) *syn*-pyramidalized 2,3-*endo,endo*-disubstituted N-acetyl 7-aza-bicyclo(2.2.1)heptanes.

The differences in interaction energy (with the N lone pair) between C-C bonds of the substituted bridge and those of the unsubstituted bridge correlate with the pyramidalization values for the 2,3-*endo,endo*-disubstituted 7-azabicyclo(2.2.1)heptyl cations and 2,3-*endo,endo*-disubstituted N-thioacetyl 7-azabicyclo(2.2.1)heptanes (Figure 23). However, the ΔIE and θ_N relationship does not seem to be general for N-acetyl 7-azabicyclo(2.2.1)heptanes. When their *syn*- and *anti*- pyramidalized structures are plotted separately, there is no correlation for the *syn*-pyramidalized structures (Figure 24).

6.1.2.2. Effect of 2,3-endo,endo-Substitution on NBO Energies of the C-C Bonds in Bicyclo(2.2.1)heptane Skeleton

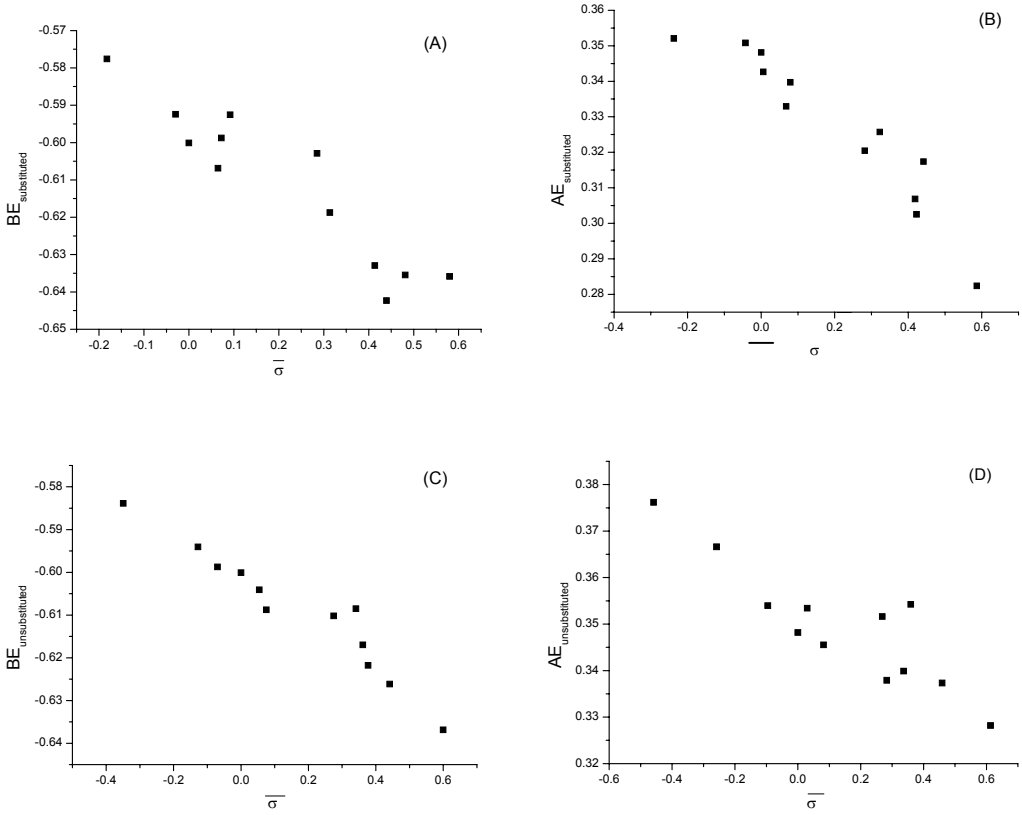

Figure 25: The energies of orbitals of C-C bonds of the 7-thioacetyl bicyclo(2.2.1)heptane (in Hartrees) vs. adjusted substituent constant, $\overline{\sigma}$. (A): bonding orbital of substituted bridge; (B) : antibonding orbital of substituted bridge; (C) : bonding orbital of unsubstituted bridge; (D): antibonding orbital of unsubstituted bridge

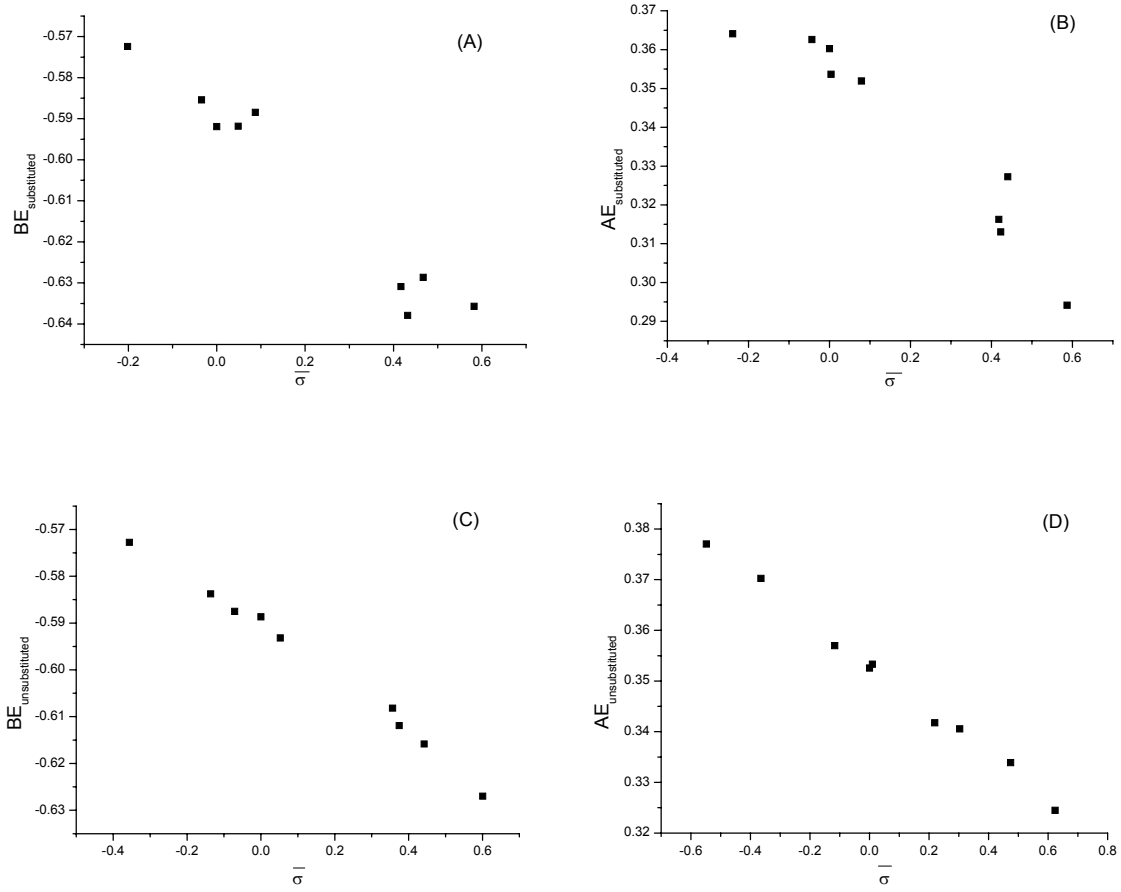

Figure 26: The energies of orbitals (in Hartrees) of C-C bonds of the syn-pyramidalized 7-acetyl bicyclo(2.2.1)heptane vs. adjusted substituent constant, $\bar{\sigma}$. (A): bonding orbital of substituted bridge; (B) : antibonding orbital of substituted bridge; (C) : bonding orbital of unsubstituted bridge; (D): antibonding orbital of unsubstituted bridge

Any parameter which correlates simultaneously with dual substituent constants can be analyzed with multiple regression analysis. For this purpose, the Hammett equation is transformed as:

$$\bar{X} = \rho_I\sigma_I + \rho_R\sigma_R = \bar{\sigma} * \rho$$

In our case, a multiple regression analysis of the energies of the bonding/ antibonding energies on dual parameters has been performed. Then using $\lambda = \rho_R / \rho_I$, $\bar{\sigma}$ values are computed and plotted against the orbital energy values. The λ values as well as slope and R values have been listed in Table 17.

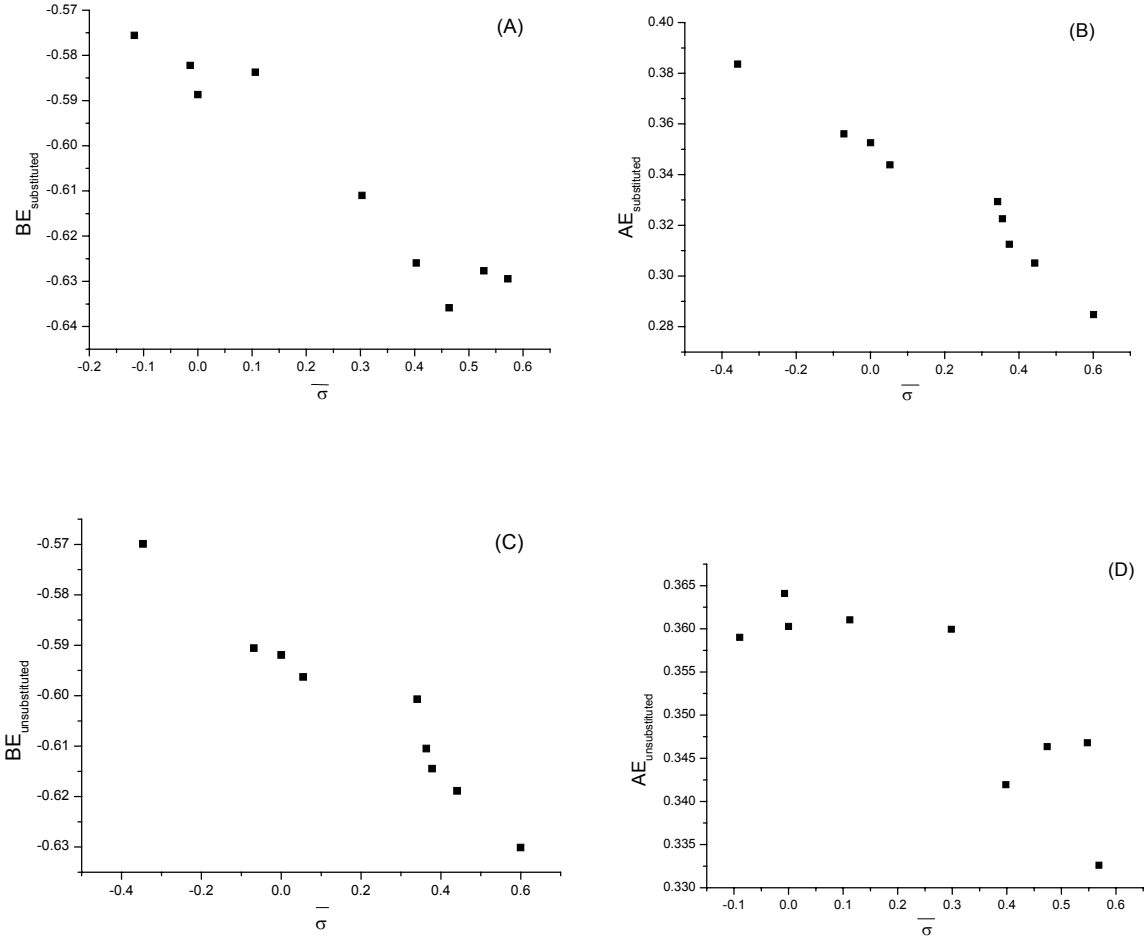

Figure 27: The energies of orbitals (in Hartrees) of C-C bonds of the *anti*-pyramidalized 7-acetyl bicyclo(2.2.1)heptane vs. adjusted substituent constant, $\overline{\sigma}$. (A): bonding orbital of substituted bridge; (B) : antibonding orbital of substituted bridge; (C) : bonding orbital of unsubstituted bridge; (D): antibonding orbital of unsubstituted bridge

Figures 25-27 show that the bonding/antibonding orbital of the unsubstituted bridge is more dependent on the resonance constants than the substituted counterparts. The slopes are found to be larger for the substituted bonds than the unsubstituted bonds. It should also be noticed that some of the substituents (NPH_3, CH_3, $CHCH_2$ and –NH-CH_2-NH-) consistently raise the bonding and antibonding energies and the others consistently lower them.

Figure No	λ	Slope	R
25A	0.12	-0.08	-0.94
25B	0.21	-0.08	-0.94
25C	0.37	-0.05	-0.96
25D	0.54	-0.04	-0.89
26A	0.15	-0.09	-0.98
26B	0.21	-0.09	-0.96
26C	0.38	-0.06	-1.00
26D	0.67	-0.04	-1.00
27A	0.03	-0.09	-0.97
27B	0.38	-0.10	-0.98
27C	0.37	-0.06	-0.97
27D	-0.02	-0.04	-0.85

Table 17: λ values and the slope and R values of the plots in Figures 25-27

6.1.2.3. Correlation of Pyramidalization at N7 with NBO Energies of the C-C Bonds

The attempt to correlate θ_N values with Δ(BD) and Δ(BD*) failed for the entire sets of thio-, and *syn* and *anti* oxo-amides. However, the N-thioacetyl 7-azabicyclo(2.2.1)heptane set is large enough to treat separately the data for the net donor substituents and for the net acceptor substituents. The separated subsets yield quite satisfactory but different results of dual parameter correlation.

Figure No	λ	R
28A	-1.00	-0.77626
28B	-0.17	-0.84481
28C	-0.92	-0.84481

Table 18: λ and R values of the plots in Figure 28

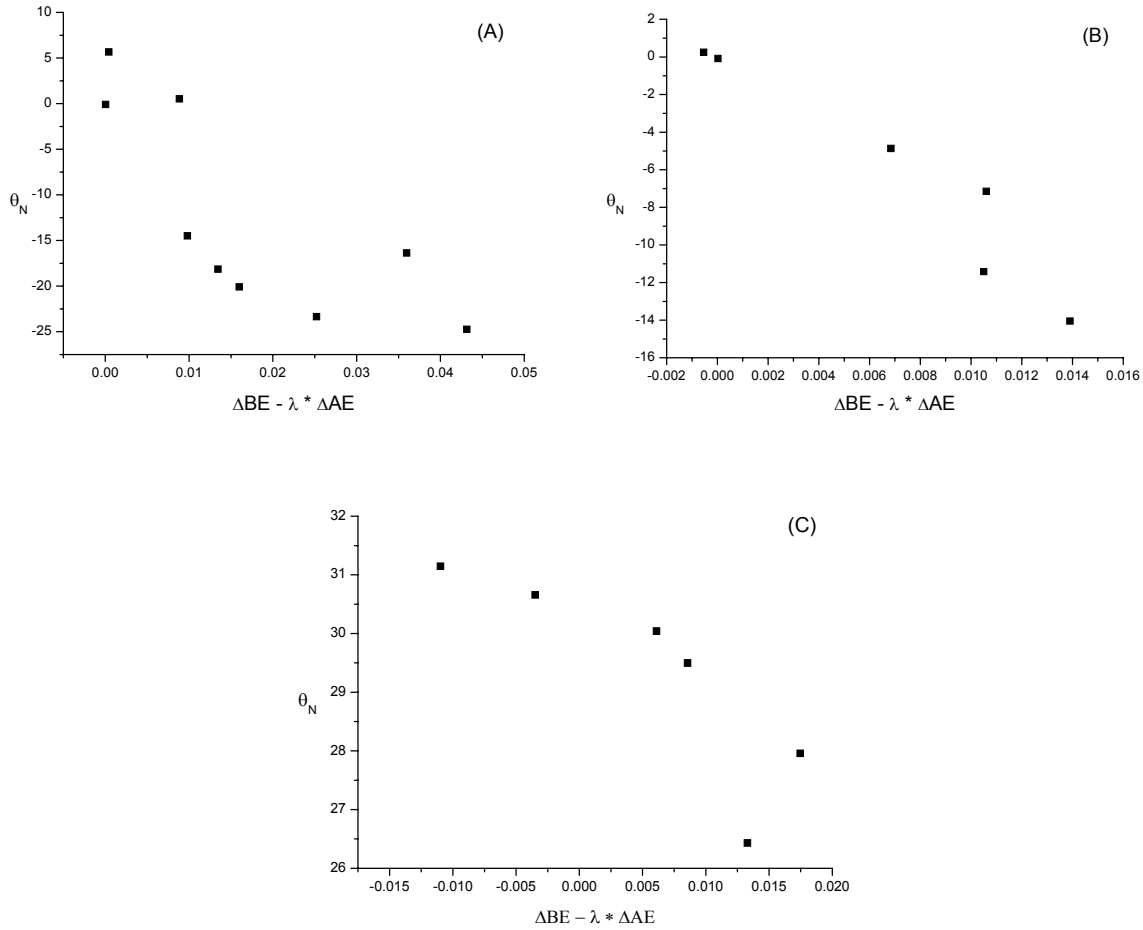

Figure 28: Correlation of pyramidalization (in degrees) with the differences in NBO energies (kcal/mol) of the C-C bonds of substituted and unsubstituted bridges

(A): N-thioacetyl 7-azabicyclo(2.2.1)heptane with acceptor substituents;

(B): N-thioacetyl 7-azabicyclo(2.2.1)heptane with donor substituents;

(C): *syn*-pyramidalized N-acetyl 7-azabicyclo(2.2.1)heptane with donor substituents

6.1.3. Effect of the Substituent Conformation

For two of the substituents included in Sections 6.1.1.1, 6.1.1.2 and 6.1.1.3, vinyl ($CHCH_2$) and $N{=}PH_3$, the effect of conformation is investigated. Comparison of the total natural charge of the substituent and amide group in different conformations informs one about the flow of electron density upon conformational changes.

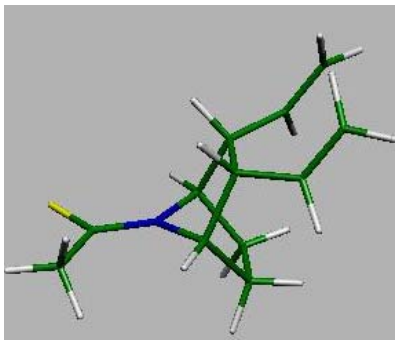

29(constrained)

vinyl charge : 0.5294 θ_N= 0.541˚

amide charge : -0.50492

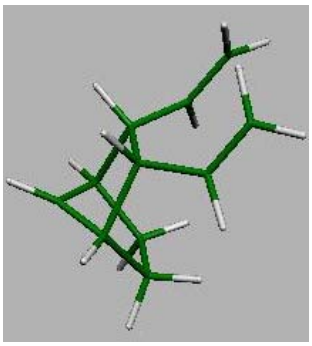

37 (constrained)

vinyl charge : 0.2100 θ_C= -16.8˚

cation charge : 0.56229

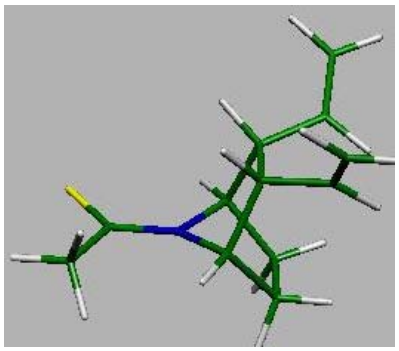

29

vinyl charge : 0.5997 θ_N= -14.047˚

amide charge : -0.50330

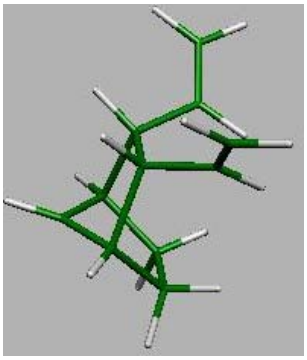

37

vinyl charge : 0.2837 θ_C= -18.3˚

cation charge : 0.51278

Scheme 43

For the vinyl substituent, the conformation has been constrained such that π-interaction between the vinyl group and the bicyclic system is unfavorable at all. And this structure is compared with the fully optimized structure in the total natural charge of the substituent and the amide group. The effect is seen in Scheme 43. When the prohibition of the π- interactions between the substituent and the bicyclic system is released, some electron

density escapes from the vinyl group to the amide (or CH^+) group for both structures **29** and **37**.

The $N{=}PH_3$ substituent has been optimized with two different constraints: one of them (**8** and **26**) makes π-interactions favorable and the other (**9** and **27**) does not allow it at all. The comparison of the natural atomic charges on the substituent, shown in Scheme 44, gives a parallel result with the vinyl group: an electron density flow from $N{=}PH_3$ to the amide when the conformation becomes suitable for interactions on going from **9** to **8** and from **27** to **26**.

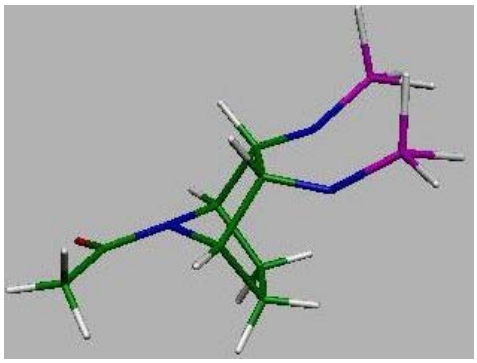

9

substituent charge : -0.30554

amide charge : -0.47140 θ_N= 27.958˚

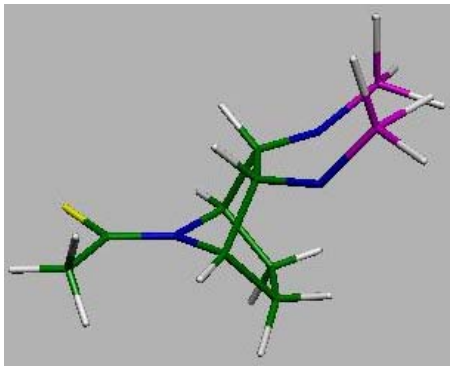

27

substituent charge : - 0.29475

amide charge : -0.52181 θ_N= -7.147˚

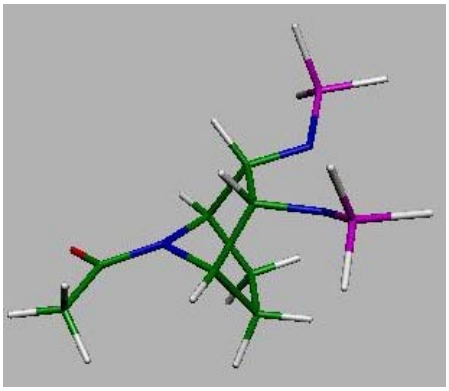

8

substituent charge : -0.24102

amide charge : -0.47528 θ_N= 26.432˚

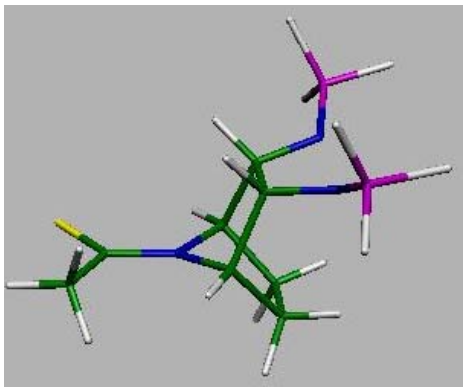

26

substituent charge : -0.22564

amide charge : -0.52790 θ_N= -11.418˚

Scheme 44

6.2. Discussion

DFT calculations (B3LYP/6-31G*) reproduce quite well the molecular geometry of N-acyl-7-azabicyclo(2.2.1)heptane in the crystal structure. In these amides, N is pyramidalized, with $\theta_N \sim 30^o$. Consequently, substitution of the bicycloheptyl skeleton yields two isomers, which are referred to here as the *anti*- and *syn*-pyramidalized acetamides. The differences in energy of those isomers are very small, too small to consider any trends related to the substituent properties. The 2,3-*endo,endo*- substitution also has a relatively small effect on the magnitude of the pyramidalization – the range of θ_N is ~10º.

The barrier to inversion in these N-acetyl-7-azabicyclo(2.2.1)heptanes appears to be minute. It is then not surprizing that in the corresponding thioamide, due to the increased π-bonding, N is virtually planar. Here, the 2,3-*endo,endo*- substitution has a considerable effect on the amide ground state geometry: θ_N varies within ~30º. Interestingly, both strongly electron-donating and –accepting substituents induce the *anti* pyramidalization, while the substituents of moderate properties tend to induce none or *syn* pyramidalization.

The comparison of these effects can be made with the substituent effects on the planarity of 7-bicyclo(2.2.1)heptyl cation. In this case, the θ_C range is similar, ~35º. However, the net donating substituents and the net withdrawing substituents have opposite effects: *anti* and *syn* pyramidalization, respectively. The term 'net donor' is used here because some electronegative groups such as ethynyl and vinyl induce the *anti* pyramidalization, apparently due to extended hyperconjugation, i.e. backdonation from their π-bonds, as the effect of conformation on the distribution of electron density suggests in the case of the latter group.

The effect of the 2,3-substitution on the equilibrium geometry at the N7 and C7 centers can be mediated by delocalization of the C-C bonds (hyperconjugation; in the case of the cation - the only vicinal interaction possible), delocalization of the N *lp* into the C-C bonds, and repulsion between the N *lp* and the C-C bonds. The difference in the energy of such interactions with the substituted and the unsubstituted C-C bonds should be related to the magnitude of the out-of-plane distortion, since the distortion is expected to determine the orbital overlap. Indeed, the scattergrams of the NBO 2nd order perturbation analysis-derived energies of the N *lp* interactions with the C-C antibonds (the differences between the substituted and the unsubstituted bonds) vs. θ_N show satisfactory albeit not general correlation. The observed relationship confirms the above expectation. The direction of pyramidalization at C7 in the cations, where the C-C bonds can only be electron donors, shows how the overlap is optimized in these interactions. Pyramidalization occurs in such a

way as to bring the $2p_z$ axis in better alignment with the better donor C-C bond. This has also been found in the computational studies of 1-methylcyclohexyl cation[106] and in the experimental ^{13}C NMR study of biadamantyl cation.[107]

To find out which vicinal interactions determine the direction of out-of-plane distortions in N-thioacetyl-7-azabicyclo(2.2.1)heptanes, one should establish whether θ_N correlates with the bond energies (if the C-C donation is important) or with the antibond energies (if the N *lp* donation is important). Dual parameter treatment and bivariate correlation fail for the entire set of the thioacetamides. However, the fact that both donating and withdrawing substituents induce the same direction of pyramidalization suggests that the major contribution may be changing with the substitution. The correlations of the bond and antibond energies with the substituent inductive and resonance effects (σ_I and σ_R constants, dual parameter treatment) reveal that the set of substituents employed in the study can be divided into the subsets of the groups that consistently raise bond and antibond energies, and those groups that consistently lower these energies. If the θ_N vs. the bond energies correlations are attempted for those two subsets separately, the results are quite satisfactory. This outcome suggests that the thioamide can indeed be not only an electron donor but also a hyperconjugative σ-electron acceptor.

This conclusion is supported by the examination of the electron density shifts that occur upon change in conformation of the vinyl and phosphoimidyl groups. In both cases, the acetamide, thioacetamide and cation have been optimized with the substituents in the constrained orientations which preclude extended hyperconjugation of the π-bond. Upon releasing the constraint, pyramidalization is found to increase in every case, and the summation of the NPA atomic charges over the substituents, and over the amide or the cation moieties, indictates the shift of charge from the substituents into the N7 or C7 center.

7. Resonance Interaction Propensities of Amino Acid Side Chains: 3- Substituted 5,6-Diaza-1-bicyclo(2.2.1)hexyl Cations

7.1. Results

5,6-Diaza-1-bicyclo(2.2.1)hexyl cations (Scheme 45) substituted with 20 coded amino acid side chains as well as a set of standard Hammett-treatment substituents at C3 have been optimized with B3LYP/6-31G* method. Frequency calculations confirm that the minimum is located in each case.

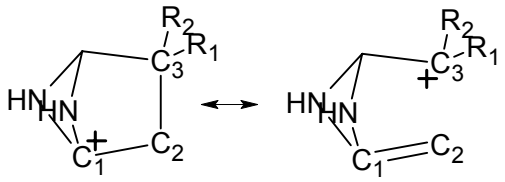

Scheme 45

7.1.1. Molecular Geometry

Upon substitution the major changes in geometry are observed for C1-C2 and C2-C3 bonds: C1-C2 bond shortens when C2-C3 bond lengthens. C1-C2 bond length has a range of 1.452-1.503 Å and C2-C3 bond has a range of 1.622–1.805 Å. In order to check whether

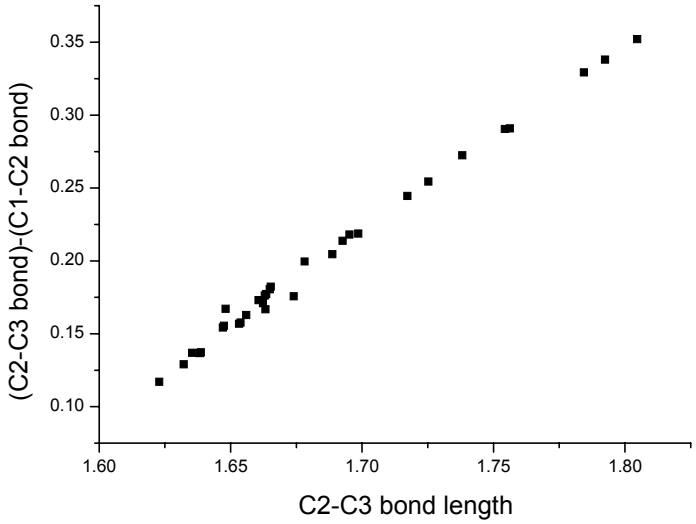

Figure 29: Difference between C1-C2 and C2-C3 bond lengths versus C2-C3 bond length

these bond length changes are due to the same effect Figure 29,which shows the relation between C2-C3 bond and the difference in the two mentioned bonds, has been prepared using 32 substituents. The plot confirms that the variation in bond distances results from the substituent effect on C2-C3 hyperconjugation.

7.1.2. NBO Analysis

The C2-C3 bond is placed at the connection of the substituent and the parent structure. Any kind of π-interaction will appear mostly on the antibonding orbital of this bond. Figure 30 shows that the occupancies of C2-C3 antibonding orbitals correlate very well with the

	σ_R	Occupancy
96	0	0.00000
104	-0.12	0.01363
120	-0.16	0.01885
112	-0.32	0.03594
113	-0.31	0.03197
117	-0.48	0.04020
118	-0.25	0.03697
119	-0.25	0.03169
107	-0.62	0.07782
110	-0.78	0.10437
127	-0.18	0.01864

Table 19: Properties of the set of 11 substituents used in initial correlation

resonance constants (σ_R) of substituents for the set of 11 substituents , that have experimental σ_R values available and are neither π- nor σ-acceptors. The σ_R values used are the experimental values obtained by Charton. A linear fit gives an equation as:

Occupancy of BD*(C2-C3) - Occupancy of BD*(C2-C3) of H, H= $-0.12617 * \sigma_R - 0.00252$

with R= -0.97128 and standard deviation= 0.00746.

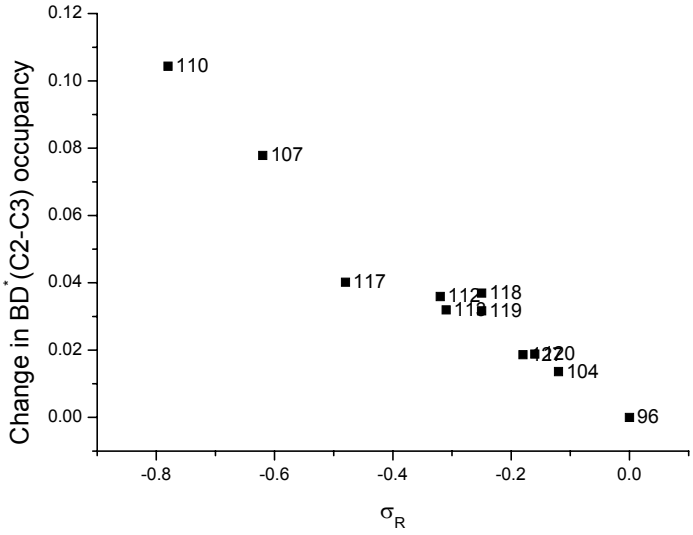

Figure 30: Correlation between occupancy of antibonding orbital of C2-C3 bond and σ_R

Based on the linear correlation shown in Figure 30, one can find σ_R value for a substituent by using the occupancy of BD*(C2-C3) orbital obtained computationally. The σ_R values calculated using this procedure for Ala* amino acid side chains are listed in Table 21 and those for the selected standard substituents in Table 20.

No	R1	R2	σ^{EH}_R
117	F	H	-0.34
118	Cl	H	-0.32
119	Br	H	-0.28
120	CH3	H	-0.11
121	CF3	H	-0.11
122	CCH	H	-0.29
123	CN	H	-0.18
124	NO2	H	-0.12
125	3-fluorobenzyl	H	-0.42
126	3-aminobenzyl	H	-0.82
127	t-Bu	H	-0.17

Table 20: The resonance constants for the selected standard substituents

aa	No	R1	R2	σ^{EH}_R
Ala	**96**	H	H	-0.02
His	**97**	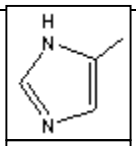	H	-0.63
His(+)	**98**	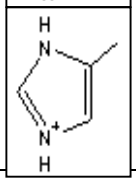	H	-0.21
Met	**99**	CH_2SCH_3	H	-0.24
Leu	**100**	$CH(CH_3)_2$	H	-0.15
Lys(+)	**101**	$CH_2CH_2CH_2NH_3^+$	H	-0.10
Glu	**102**	CH_2CO_2H	H	-0.12
Glu(-)	**103**	$CH_2CO_2^-$	H	-0.41
Gln	**104**	CH_2CONH_2	H	-0.13
Asp	**105**	CO_2H	H	-0.07
Asp(-)	**106**	CO_2^-	H	-0.21
Ser	**107**	OH	H	-0.64
Asn	**108**	$CONH_2$	H	-0.08
Trp	**109**	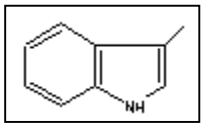	H	-0.71
Thr	**110**	CH_3	OH	-0.85
Cys	**111**	SH	H	-0.50
Val	**112**	CH_3	CH_3	-0.30
Ile	**113**	CH_2CH_3	CH_3	-0.27
Arg(+)	**114**	$CH_2CH_2NHC(NH_2)_2(+)$	H	-0.09
Phe	**115**	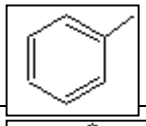	H	-0.38
Tyr	**116**	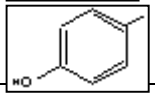	H	-0.57

Table 21: The resonance constants for Ala* amino acid side chains

7.2. Discussion

In the course of an extensive search for an appropriate model cation, 5,6-diaza-1-bicyclo(2.1.1)hexyl cation turned out to be unique in the sensitivity of its structure to extended hyperconjugation effects, and in its stability allowing to examine C3 substituents of a wide range of properties, in particular all the coded amino acid side chains including their ionized forms. As implied by the bond-no bond resonance representation of the C2-C3 hyperconjugation in this cation, elongation of the C2-C3 bond should be accompanied by shortening of the C1-C2 bond. The excellent correlation between the C2-C3 bond distance and the difference in the C1-C2 and C2-C3 bond distances, including even the charged substituents, demonstrates that hyperconjugation is by far the most important process here, dominating structural variation in these cations and mediating the effect of substitution on the cation structure.

The capacity of the substituents as π-donors can in principle be characterized by the amount of charge transferred to an acceptor fragment. In the present model cation, the substituent charge is transferred into the C2-C3 bond. The NBO analysis allows to examine the occupancies of the localized bonding and antibonding orbitals associated with this bond. Serendipitously, the latter is engaged in very little interaction within the cation, and its occupancy in the parent structure is near zero. Thus, the occupancies of this orbital in the substituted cations can be taken as a measure of the substituent's π-donor capacity. Indeed, these occupancies correlate very well with the available experimental σ_R constants for the substituents that cannot act as acceptors towards the benzene ring, i.e. their resonance effect in the aromatic derivatives is due to the density shift in one direction only. The observed correlation offers then a convenient way to quantify the resonance capacity of any substituent that can be attached at C3 without breaking up the cation. For the first time, the constants that characterize resonance interactions in the σ-bond systems are obtained, and placed on the scale of the conventional experimental σ_R constants. This result is particularly important for examining the contribution of hyperconjugation between the amino acid side chains and the peptide linkages to the local interactions in proteins.

8. Summary

Effects of substitution have been characterized by computational examination of the changes in energy, molecular geometry, electron density distribution, and electronic structure, in three series of compounds: (1) formamides $HC(=X)NY_2$ (X=O, S, Se; Y=H, CH_3, F, Cl, Br); (2) 2,3,-*endo,endo*-disubstituted N-acyl-7-azabicyclo(2.2.1)heptanes and 2,3,-*endo,endo*-disubstituted 7-bicyclo(2.2.1)-heptyl cations; and (3) 3-substituted 5,6-diaza-1-bicyclo-(2.1.1)hexyl cations. Both *ab initio* (MP2) and DFT methods were employed using Pople's basis sets (6-31+G(2d), 6-31+G* and 6-31G*).

The effect of N-halo substitution on the potential energy surface of simple formamide derivatives is found to be largely related to the electronegativity of the substituents. The exception to this general trend is found in the case of the fluorine substitution in the transition structures for inversion, where donation from the fluorine *lp* appears to assist π-bonding across the C-N bond, stabilizing the charge polarized resonance form of the amide group. This is supported by the examination of the variation in bond distances, bond orders, energies and extensions of the canonical π-symmetry orbitals, and occupancies of the NBOs. On the other hand, the implied π-bonding across the N-F bond is not reflected in group-transfer energies obtained as heats of isodesmic substitution reactions, the effect being apparently too small in comparison to total bond energies.

In accordance with experimental data, N-acetyl-7-azabicyclo(2.2.1)heptane is found to be highly pyramidalized at N7. However, due to the very small barrier of inversion, chalcogen substitution, as in N-thioacetyl and N-selenoacetyl- derivatives, results in virtual planarity of the amide N. The planar geometry is readily distorted by remote substitution in 2,3-*endo,endo*-disubstituted N-thioacetyl-7-azabicyclo(2.2.1)-heptanes. The direction of the pyramidalization is the same for strongly electron-donating substituents and strongly electron-withdrawing substituents. Dual parameter treatment suggests that in the first case pyramidalization depends largely on the NBO energies of the occupied orbitals of the bicycloheptane C-C bonds, while in the second case both the occupied and vacant orbitals interact with the N center. Examination of electron density shifts associated with the change in conformation of the π-donor substituents confirms that the thioamide N acts as a resonance acceptor of the σ C-C density.

Finally, the 5,6-diaza-1-bicyclo(2.1.1)hexyl cation is found to be an excellent model system to probe the π-donor capacity of a range of substituents, including all the coded amino

acid side chains, even in their ionized forms. The first scale of substituent constants is obtained to characterize resonance interactions in the σ-bond systems, related to the scale of conventional experimental σ_R constants.

The findings of the present study suggest that the amide linkage can indeed act as a resonance acceptor of π- and σ-density of its N substituents. These results may further our understanding of the local interactions in proteins and the origin of secondary structure propensities of the coded amino acids.

9. References:

1. Bent, H. A. *Chem. Rev.* **1968**, *68*, 587.
2. Pauling, L. *The Nature of the Chemical Bond*, 3rd ed.; Cornell University Press: Ithaca, NY, 1960; pp. 281-282.
3. a. Wiberg, K. B.; Laidig, K. E. *J. Am. Chem. Soc.* **1987**, *109*, 5935;
   b. Wiberg, K. B.; Breneman, C. M. *J. Am. Chem. Soc.* **1992**, *114*, 1960.
4. Glendening, E.D.; Hrabal II, J.A. *J. Am. Chem. Soc.* **1997**,119,12940-12946
5. Perrin, C. L. *J. Am. Chem. Soc.* **1991**, *113*, 2865.
6. Cieplak, A. S. *Struct. Chem.* **1994**, *5*, 85.
7. a. Honig, B.; Cohen, F. E. *Folding Des.* **1996**, *1*, R17; b. Srinivasan, R.; Rose, G. D. *Proc. Natl. Acad. Sci. U.S.A.* **1999**, *96*, 14258; c. Zitzewitz, J. A.; Ibarra-Molero, B.; Fishel, D. R.; Terry, K. L.; Matthews, C. R. *J. Mol. Biol.* **2000**, *296*, 1105; d. Moran, L. B.; Schneider, J. P.; Kentisis, A.; Reddy, G. A.; Sosnick, T. R. *Proc. Natl. Acad. Sci. U.S.A.* **1999**, *96*, 10699; e. Dill, K. A. *Biochemistry* **1990**, *29*, 7133; f. Honig, B.; Yang, A.- S. *Adv. Protein Chem.* **1995**, *46*, 27; g. Murphy, K. P.; Gill, S. J. *J. Mol. Biol.* **1990**, *222*, 699; h. Honig, B. *J. Mol. Biol.* **1999**, *293*, 283; i. Doig, A. J.; Williams, D. H. *J. Am. Chem. Soc.* **1992**, *114*, 338; j. Pace, C. N.; Shirley, B. A.; McNutt, M.; Gajiwala, K. *FASEB J.* **1996**, *10*, 75; k. Rose, G. D.; Wolfenden, R. *Ann. Rev. Biophys. Biomol. Struct.* **1993**, *22*, 381; l. Dado, G.; Gellman, S. H. *J. Am. Chem. Soc.* **1993**, *115*, 4228.
8. Cordier, F.; Grzesiek, S. *J. Am. Chem. Soc.* **1999**, *121*, 1601.
9. Cornilescu, G.; Hu, J.-S.; Bax, A. *J. Am. Chem. Soc.* **1999**, *121*, 2949.
10. Cornilescu, G.; Ramirez, B. E.; Frank, M. K.; Clore, G. M.; Gronenborn, A. M.; Bax, A. *J. Am. Chem. Soc.* **1999**, *121*, 6275.
11. Juranić, N.; Macura, S. *J. Am. Chem. Soc.* **2001**, *123*, 4099.
12. Baker, E. N.; Hubbard, R. E. *Prog. Biophys. Mol. Biol.* **1984**,44,97
13. Harris, T. K.; Mildvan, A. S. *Proteins: Struct., Funct., and Genet.* **1999**, *35*, 275.
14. Kubelka, J.; Keiderling, T. A. *J. Am. Chem. Soc.* **2001**, *123*, 12048.
15. Wintrode, P. L.; Makhatadze, G. I.; Privalov, P. L. *Proteins: Struct., Funct., and Genet.* **1994**, *18*, 246.
16. Koh, J. T.; Cornish, V. W.; Schultz, P. G. *Biochemistry* **1997**, *36*, 11314.
17. Chapman, E.; Thorson, J. S.; Schultz, P. G. *J. Am. Chem. Soc.* **1997**, *119*, 7151.
18. Beligere, G. S.; Dawson, P. E. *J. Am. Chem. Soc.* **2000**, *122*, 12079.
19. Nakhle, B. M.; Silinski, P.; Fitzgerald, M. C. *J. Am. Chem. Soc.* **2000**, *122*, 8105.

20. Wales, T.E.; Fitzgerald, M. C. *J. Am. Chem. Soc.* **2001**, *123*, 7709.
21. a. Mendel, D.; Cornish, V. W.; Schultz, P. G. *Annu. Rev. Biophys. Biomol. Struct.* **1995**, *24*, 435; b. Muir, T. W.; Kent, S. B. H. *Curr. Opin. Biotechnol.* **1993**, *4*, 420.
22. Cieplak, A. S. in preparation.
23. Cornilescu, G.; Bax, A.; Case, D. A. *J. Am. Chem. Soc.* **2000**, *122*, 2168.
24. Contreras, R. H.; Peralta, J. E. *Progr. NMR Spectrosc.* **2000**, *37*, 321.
25. Cieplak, A. S. in *The Amide Linkage: Selected Structural Aspects in Chemistry, Biochemistry, and Materials Science* © **2000** John Wiley & Sons; Chapter 17, p. 565.
26. Wiberg, K. B.; Hammer, J. D.; Keith, T. A.; Zilm, K. *Tetrahedron Lett.* **1997**, *38*, 323.
27. Minor, D. L. Jr; Kim, P. S. *Nature* **1994**, *367*, 660.
28. Smith, C. K.; Withka, J. M.; Regan, L. *Biochemistry* **1994**, *33*, 5510.
29. Minor, D. L. Jr; Kim, P. S. *Nature* **1994**, *371*, 264.
30. Cieplak, A. S. *Chem. Rev.* **1999**, *99*, 1265.
31. Wiberg, K. B.; Rablen, P. R. *J. Org. Chem*. **1998**, 63, 3722
32. Glushka, J.; Lee, M.; Coffin, S.; Cowburn, D. *J. Am. Chem. Soc.* **1990**, *112*, 2843; see also: Braun, D.; Wider, G.; Wütrich, K. *J. Am. Chem. Soc.* **1994**, *116*, 8466; Schwarzinger, S.; Kroon, G. J. A.; Foss, T. R.; Chung, J.; Wright, P. E.; Dyson, H. J. *J. Am. Chem. Soc.* **2001**, 123, 2970
33. Dunitz, J.D.; Winkler, F. K. *Acta Crystallogr.* **1975**, B31, 251
34. Brown, R.D.; Godfrey, P. D.; Kleibomer, B. *J. Mol. Spectrosc.* **1987**, *124*, 34
35. Stevens, E. D. *Acta Crystallogr.* **1978**, B34, 544
36. Hirota, E.; Sugisaki, R.; Nielsen, C. J.; Sorensen, G. O. *J. Mol. Spectr.* **1974**, *49*, 251
37. Schultz, G.; Hargittai, I. *J. Phys. Chem.* **1993**, *97*, 4966
38. Schultz, G.; Hargittai, I. *J. Phys. Chem.* **1995**, *99*, 11412
39. Kitano, M.; Kuchitsu, K. *Bull. Chem. Soc. Japan* **1974**, *47(3),* 631
40. Kitano, M.; Fukuyama, T.; Kuchitsu, K. *Bull. Chem. Soc. Japan* **1973**, *46*, 384
41. Sugisaki, R.; Tanaka, T.; Hirota, E. *J. Mol. Spectrosc.* **1974**, *49*, 241
42. Neugebauer Crawford, S. M.; Taha, A. N.; True, S. N. *J. Phys. Chem. A* **1997**, *101*, 4699
43. Bennet, A.J.; Somayaji, V.; Brown, R. S.; Santarsiero, B. D. *J. Am. Chem. Soc.* **1991**, *113*, 7563
44. Ross, B. D.; True, N. S.; Matson, G. B. *J. Phys. Chem.* **1984**, *88*, 2675
45. Ross, B. D.; True, N. S. *J. Am. Chem. Soc.* **1984**, *106*, 2451
46. Taha, A. N.; Neugebauer Crawford, S. M.; True, N. S. *J. Am. Chem. Soc.* **1998**, *120*, 1934
47. Feigel, M. *J. Phys. Chem.* **1983**, *87*, 3054

48. Wiberg, K. B.; Rablen, P. R.; Rush, D. J.; Keith, T. A. *J. Am. Chem. Soc.* **1995**, *117*, 4261

49. Cox, C.; Leckta, T. *J. Org. Chem.* **1998**, *63*, 2426

50. a) Tichy, M.; Duskova, E.; Blaha, K. *Tetrahedron Lett.* **1974**,237;
b) Greenberg, A.; Chiu, Y. -Y.; Johnson, J. L.; Liebman, J. F. *Struct. Chem.* **1991**, *2*, 117

51. Pracejus, H.; Kehlen, M.; Kehlen, H.; Matschiner, H. *Tetrahedron* **1965**, *21*, 2257

52. Bernardi, F.; Lunazzi, L.; Zanirato, P.; Cerioni, G. *Tetrahedron* **1977**, *33*, 1337

53. Fong, C. W.; Grant, H. G. *Aust. J. Chem.* **1981**, *34*, 2307

54. a) Treschanke, L.; Rademacher, P. J. *J. Mol. Struct.* **1985**, *122*, 47
b) Greenberg, A.; Thomas, T.D.; Bevilacqua, C. R.; Coville, M.; Ji, D.; Tsai, J.-C.; Wu, G., *J. Org. Chem.* **1992**, *57*, 7093

55. Wiberg, K. B.; Hadad, C. M.; Rablen, P. R.; Cioslowski, J. *J. Am. Chem. Soc.* **1992**, *114*, 8644

56. Wiberg, K. B.; Rablen, P. R. *J. Am. Chem. Soc.* **1993**, *115*, 9234

57. Laidig, K. E.; Cameron, L. M. *Can. J. Chem.* **1993**, *71*, 872

58. Wiberg, K. B.; Rablen, P. R. *J. Am. Chem. Soc.* **1995**, *117*, 2201

59. Laidig, K. E.; Cameron, L. M. *J. Am. Chem. Soc.* **1996***, 118*, 1737

60. Bader, R. F. W. *Atoms In Molecules: A Quantum Theory;* Clarendon Press Oxford, U.K., **1990**

61. a) Foster, J. P.; Weinhold, F. J. *J. Am. Chem. Soc.* **1980**,*102*,7211;
b) Reed, A. E.; Curtiss, L. A.; Weinhold, F. *Chem. Rev.* **1988**, 88, 899;
c) Reed, A. E.; Weinstock, R. B.; Weinhold, F. *J. Chem. Phys.* **1985**, 83, 735

62. a) Glendening, E. D. Ph.D. Thesis, University of Wisconsin, Madison, WI, **1991**;
b) Glendening, E. D.; Weinhold, F. *J. Comput. Chem.* **1998**, 19, 593

63. Ohwada, T.; Achiwa, T.; Okamoto, I.; Shudo, K. *Tetrahedron Lett.* **1998**, 39, 865

64. Ohwada, T.; Okamoto, I.; Shudo, K.; Yamaguchi, K. *Tetrahedron Lett.* **1998**, 39, 7877

65. Blanca, M. B.- D.; Maimon, E.; Kost, D. *Angew. Chem. Int. Ed. Engl.* **1997**, 36,2216

66. Miura, M.; Sakamoto, S.; Yamaguchi, K.; Ikeda, H.; Ohwada, T. *J. Am. Chem. Soc.* **2000**, *41*, 3637

67. Ohwada, T.; Miura, M.; Tanaka, H.; Sakamoto, S.; Yamaguchi, K.; Ikeda, H.; Inagaki, S. *J. Am. Chem. Soc.* **2001**, *123*, 10164

68. Mannschreck, A.; Munsch, H.; Mattheus, A. *Angew. Chem. Int. Ed. Engl.* **1966**, *5*, 728

69. Mannschreck, A.; Munsch, H. *Angew. Chem. Int. Ed. Engl.* **1967**, *6*, 984

70. Gropen, O.; Skancke, P. N. *Acta Chem. Scand.* **1971**, *25*, 1241

71. Gdaniec, M.; Milewska, M. J.; Polonski, T. *J. Org. Chem.* **1995**, *60*, 7411
72. Cooney, J. D.; Brownstein, S. K.; Apsimon, J.W. *Can. J. Chem.* **1974**, *52*, 3028
73. Harris, R. K.; Pryce-Jones, T.; Swinbourne, F. J. *J. Chem. Soc, Perkin Trans. 2* **1980**, 476
74. Mehta, G.; Khan, F. A. *J. Am. Chem. Soc.* **1990**, *112*, 6140
75. Li, H.; Mehta, G.; Padma, S.; le Noble, W. J. *J. Org. Chem.* **1991**, *56*, 1006
76. Mehta, G.; Praveen, M. *Tetrahedron Lett.* **1992**, *33*, 1759
77. Mehta, G.; Khan, F. A.; Adcock,W. J. *J. Chem. Soc., Perkin Trans. 2* **1995,** 2189
78. Mehta, G.; Khan, F. A.; Mohal, N.; Narayan Namboothiri, I. N.; Kalyanaraman, P.; Chandrasekhar, J. *J. Chem. Soc., Perkin Trans. 1* **1996**, 2665
79. Keseru, G. M.; Kajtar- Peredy, M.; Naray- Szabo, G. *Tetrahedron Lett*. **1994**, *35*, 9255
80. Mehta, G.; Khan, F. A.; Ganguly, B.; Chandrasekhar, J. *Chem. Soc., Perkin Trans. 2* **1994**, 2275
81. Ganguly, B.; Chandrasekhar, J.; Khan, F. A.; Mehta, G. *J. Org. Chem.* **1993**, *58*, 1734
82. Mehta, G.; Khan, F. A. *J. Chem. Soc., Chem. Commun*. **1991**, 18
83. Paddon- Row, M. N.; Wu, Y.-D.; Houk, K. N. *J. Am. Chem. Soc*. **1992**, *114*, 10638
84. Yadav, V. K. *J. Org. Chem*. **2001**, *66*, 2501
85. Yadav, V. K.; Balamurugan, R. *J. Chem. Soc., Perkin Trans. 2* **2001**,1
86. Yadav, V. K.; Balamurugan, R. *J. Org. Chem.* **2002**, *67*, 587
87. Lambert, J.B. *Tetrahedron* **1990**, *46*, 2677
88. Lambert, J. B.; Wang, G.; Teramura, D. H. *J. Org. Chem*. **1988**, *53*, 5422
89. Lambert, J. B.; Salvador, L. A.; So, J -H. *Organometallics* **1993**, *12*, 697
90. Lambert, J. B.; Ciro, S. M. *J. Org. Chem*. **1996**, *61*, 1940
91. Senda, Y.; Morita, M.; Itoh, H. *J. Chem. Soc., Perkin Trans.2* **1996**, 221
92. Mehta, G.; Khan, F. A.; Garde, S. R.; Shirsat, R. N.; Ganguly, B.; Chandrasekhar, J. *Angew. Chem. Int. Ed. Engl.* **1994**, *33*, 1390
93. a) Raber, D. Jr.; Neal, W. C. Jr.; Dukes, M. D., Harris, J. M.; Mount, D.L. *J. Am. Chem. Soc.* **1978**, *100*, 8137;
b) Harris, J. M.; Mount, D. L.; Smith, M. R.; Neal, W. C. Jr.; Dukes, M. D.; Raber, D. J. *J. Am. Chem. Soc*. **1978**, *100*, 8147
94. Mehta, G.; Chandrasekhar, J. *Chem. Rev.* **1999**, *99*, 1437
95. Aggarwal, V. K.; Ford, J. G.; Fonquerna, S.; Adams, H.; Jones, R. V. H.; Fieldhouse, R. *J. Am. Chem. Soc.* **1998***, 120*, 8328
96. Laube, T. *Angew. Chem. Int. Ed. Engl.* **1986**, *25*, 349
97. Laube, T.; Schaller, E. *Acta Crystallogr., Sect. B* **1995**, B51, 177

98. Allen, F. H.; Kennard, O.; Watson, D. G.; Brammer, L.; Orpen, G.; Taylor, R. *In International Tables for Crystallography, Volume C*; Carlson, A. J. C., Ed.; Kluwer Academic Publishers: Dordrecht, **1992**; 685-706

99. Laube, T. *Angew. Chem. Int. Ed. Engl.* **1987**, *26*, 560

100. Laube, T. *Helv. Chim. Acta* **1994**, *77*, 943

101. Gaussian 98, Revision A.3; Frisch, M. J.; Trucks; G. W.; Schlegel, H. B.; Scuseria, G. E.; Robb, M. A.; Chieseman, J. C.; Dapprich, S.; Millem, J. M.; Daniels, A. D.; Kudin, K. M.; Strain, M. C.; Varkas, O.; Tomasi, J.; Barone, V.; Cossi, M.; Camme, R.; Mennucci, B.; Pomelli, C.; Adamo, C.; Clifford, S.; Ochterski, J.; Petersson, G. A.; Ayala, P. Y.; Cui, Q.; Morokuma, K.; Malick, D. K.; Rabuck, A. D.; Raghavachari, K.; Foresman, J. B.; Cioslowski, J.; Ortiz, J. V.; Stefanov, B. B.; Liu, G.; Liashenko, A.; Piscorz, P.; Komaromi, I.; Gompertz, R.; Martin, R. L.; Fox, D. J.; Keith, T.; Al-Laham, M. A.; Peng, C. Y.; Nanayakkara, A.; Gonzalez, C.; Challacombe, M.; Gill, P. M. W.; Johnson, B.; Chen, W.; Wong, M. W.; Andres, J. L.; Head-Gordon, M.; Replogle, E. S.; Pople, J. A.; Gaussian, Inc.: Pittsburgh PA **1998**

102. NBO 3.0; Glendening, E. D.; Reed, A. E.; Carpenter, J. E.; Weinhold, F.

103. MOLEKEL 4.0; Flükiger, P.; Lüthi, H. P.; Portmann, S.; Weber, J. Swiss Center of Scientific Computing, Manno (Switzerland), **2000**.

104. Schaftenaar, G. and Noordik, J. H. *J. Comput.-Aided Mol. Design* **2000**, *14*, 123

105. Hehre, W. J.; Ditchfield, R.; Radom, L.; Pople, J. A. *J. Am. Chem. Soc.* **1970**, *92*, 4796

106. Rauk, A.; Sorensen, T. S.; Maerker, C.; de M. Carneiro, J. W.; Sieber, S.; Schleyer, P. v. R. *J. Am. Chem. Soc.* **1996**, *118*, 3761

107. Olah, G. A.; Surya Prakash, G. K.; Shih, J. G.; Krishnamurthy, V. V.; Mateescu, G. D.; Liang, G.; Sipos, G.; Buss, V.; Gund, T. M.; Schleyer, P. v. R. *J. Am. Chem. Soc.* **1985**, *107*, 2764

108. Bent, H. A. *Chem.Rev.* **1961**, *61*, 275

109. a) Hohenberg, P. ; Kohn, W. *Phys. Rev.* **1964**, *136*, B864
b) Kohn, W. ; Sham, L. J. *Pys. Rev.* **1965**, *140*, A1133
c) Becke, A. D. *Phys. Rev. A* **1988**, *38*, 3098
d) Becke, A. D. *J. Chem. Phys.* **1993**, *98*, 1372
e) Becke, A. D. *J. Chem. Phys.* **1993**, *98*, 5648

110. a) Moller, C. ; Plesset, M. S. *Phys. Rev.* **1934**, *46*, 618
b) Pople, J. A. ; Seeger, R. ; Krishnan, R. *Int. J. Quantum Chem., Symp*., **1977**, *11*, 149
c) Pople, J. A. ; Binkley, J. S. ; Seeger. R. *Int. J. Quantum Chem., Symp*., **1977**, *10*, 1